ALTERNATIVES TO THE EFFECTIVE DOSE FOR STOCHASTIC RISK ASSESSMENT IN MEDICAL IMAGING

By

ANDRES F. ABADIA

A THESIS PRESENTED TO THE GRADUATE SCHOOL
OF THE UNIVERSITY OF FLORIDA IN PARTIAL FULFILLMENT
OF THE REQUIREMENTS FOR THE DEGREE OF
MASTER OF SCIENCE

UNIVERSITY OF FLORIDA

2012

To God, for allowing me to fulfill my dreams and giving me the strength to do so, and to my family and wife who always support and encourage me to give my best in all that I do

ACKNOWLEDGMENTS

I thank my advisor, Dr. Wesley E. Bolch, for his guidance, support, and encouragement over the last three years of my studies and for his motivation for me to start graduate school. The doors of his office were always open to me and he was always willing to help. I thank him for entrusting me with this project and having the patience to guide me through it. I would also like to thank Dr. David Pawel from the US EPA (Radiation Protection Division) for all his support and around-the-clock help with my thesis project; I thank him for teaching me how to code the models necessary to support this paper and having the patience to explain every detail of such arduous task. Finally, I would like to thank Mike Wayson and Daniel Long, from the ALRADS (Advanced Laboratory for Radiation Dosimetry Studies) group of the Biomedical Engineering department at the University of Florida, for helping me with the dosimetry for the medical example (simulation) analyzed on this paper.

TABLE OF CONTENTS

LIST OF TABLES

LIST OF FIGURES

LIST OF ABBREVIATIONS

AP	Anterior-Posterior. When referring to the medical imaging
BEIR VII	Biological Effects of Ionizing Radiation VII
C3	Committee 3
CI	Confidence Interval
CLL	Chronic Lymphocytic Leukemia
CNS	Central Nervous System
COMB	Combined
CT	Computed Tomography
DDREF	Dose and Dose Rate Effectiveness Factor
EAR	Excess Absolute Risk. The risk of disease in an exposed population minus the rate of disease in an unexposed population
EPA	Environmental Protection Agency
ERR	Excess Relative Risk. The rate of disease in an exposed population divided by the rate of disease in an unexposed population minus 1
FDG	Fludeoxyglucose (F-18). A radiopharmaceutical used in medical imaging modality PET
Gy	Gray
ICRP	International Commission on Radiological Protection
LAR	Lifetime Attributable Risk
LET	Linear Energy Transfer
LSS	Life Span Study
MRI	Magnetic Resonance Imaging
NCRP	National Council on Radiation Protection and Measurements
PA	Posterior-Anterior. When referring to the medical imaging
PET	Positron Emission Tomography

RBE	Relative Biological Effectiveness
SEER	Surveillance, Epidemiology, and End Result
Sv	Sievert
TOT	Total
UNSCEAR	United Nations Scientific Committee on the Effects of Atomic Radiation

Abstract of Thesis Presented to the Graduate School
of the University of Florida in Partial Fulfillment of the
Requirements for the Degree of Master of Science

ALTERNATIVES TO THE EFFECTIVE DOSE FOR STOCHASTIC RISK ASSESSMENT IN MEDICAL IMAGING

By

Andres Abadia

May 2012

Chair: Wesley E. Bolch
Major: Biomedical Engineering

In 2005, the BEIR (Biological Effects of Ionizing Radiation) Committee of the U.S. National Academy of Sciences published its 7th report (BEIR VII) on models for estimating risks of cancer incidence and mortality following exposure to low-LET (Linear Energy Transfer) radiation. These models take into account the subject's sex, age at exposure, dose rate and other factors. In that report, estimates for lifetime attributable risks (LAR) are given for all solid cancers, leukemia, and specific solid cancer sites. The Committee used excess relative risk (ERR) and excess absolute risk (EAR) models to project radiogenic cancer risks that are unique to the U.S. population. For most cancer sites, the Environmental Protection Agency (EPA) uses BEIR VII models for calculating lifetime attributable risks, but with some modifications and extensions. The latter include models for calculating risks for high-LET radiation exposures, and the inclusion of additional cancer sites not considered in the BEIR VII report. In this study, the revised EPA risk models have been implemented for the purpose of providing age and gender dependent LAR tables needed to better quantify stochastic risk in medical imaging studies such as computed tomography, fluoroscopy, and nuclear medicine. This approach to risk quantification is contrasted, via an FDG PET/CT medical imaging simulation example, to the use

of the ICRP (International Commission on Radiological Protection) effective dose, a quantity with limited application to medical radiation exposure of individual patients.

CHAPTER 1
INTRODUCTION

Stochastic Risks in Medical Imaging

The U.S. population is exposed to ionizing radiation – any radiation displacing electrons from atoms or molecules, thereby producing ions (*1*) – from a number of different sources. Being exposed to ionizing radiation may lead to cellular damage, which, if not adequately repaired, may prevent the survival (or reproduction) of the cell or possibly result in a change or mutation. The two outcomes, whether death or mutation of the cell occurs, have significantly different implications. These implications can be summarized best by two concepts: deterministic effects and stochastic effects. A deterministic effect is a biological effect for which its severity in affected individuals varies with the dose, and for which a dose threshold usually exists. Above the dose threshold, the severity of the effect increases with increasing dose (*1*). A stochastic effect is an effect for which the probability of its occurrence, rather than its severity, increases with increasing radiation dose. Conservatively, stochastic effects are considered to have no dose threshold (*1*).

Carcinogenesis (initiation of cancer formation) and hereditary effects fall into the category of stochastic effects. Consider for the moment a collection of somatic cells – any cell other than a germ cell that constitutes the body of an organism and that possesses a set of multiploid chromosomes (*1*) – were exposed to ionizing radiation. The probability these exposed cells will initiate cancer formation increases with the radiation dose delivered (without a dose threshold) but the severity of the cancer is not related to dose. In other words, carcinogenesis that resulted from exposure to 1 gray (Gy) is no worse than one resulting from exposure to 0.1 Gy; however, the probably of induction is increased at the higher dose level. If, on the other hand, the radiation exposure resulted in damage to a germ cell, mutations may occur that could cause harmful

effects in future generations since germ cells give rise to gametes which are cells that fuse with another cell during fertilization. Again, the severity of hereditary effects is not related to dose, but only its probability of occurrence.

These situations illustrate why we are concerned about stochastic risks in medical imaging. Radiation doses delivered as part of diagnostic imaging procedures, excluding doses resulting from accidents or interventional procedures, typically do not exceed threshold doses that would make the risks from these procedure deterministic; the potential harmful effects of diagnostic imaging are thus stochastic (either carcinogenesis or hereditary) in nature.

Furthermore, this thesis focuses only on radiogenic (radiation induced) cancer stochastic risks (from here on referred to simply as risks) and not hereditary bio-effects. To support this decision, the following statement by Dr. David J. Brenner on an article published in the British Journal of Radiology in 2008 is presented: "Although inclusion of hereditary risks was reasonable in the context of what was known in the 1970s, our current understanding is that radiation induced hereditary risks are much smaller than the corresponding cancer risks." (*2*) Dr. Brenner asserts that there is "an essential impossibility of combining cancer and hereditary risks into a single number. . . ." (*2*) For a more detailed analysis refer to the article (on the LIST OF REFERENCES).

Medical Imaging in the Past Two Decades

As mentioned earlier, the U.S. population is exposed to ionizing radiation from different sources. The sources of interest for this paper are computed tomography (CT), conventional radiography and fluoroscopy, interventional fluoroscopy, and nuclear medicine. Before trying to understand the need to quantify stochastic risks in medical imaging, it is important to glance at how these procedures have evolved in the past two decades and what role they play in today's society, and how that role affects the risk of radiogenic cancers in the U.S. population.

Computed Tomography Imaging

Publicly introduced in 1972, computed tomography (CT) has evolved into an essential diagnostic imaging tool that continues to increase in its range of clinical applications. According to the National Council on Radiation Protection and Measurements Report No. 160 (NCRP 160), technological advances in CT and the ease of use that comes with such advances, have led to an annual increased use of CT of 8 to 15% per year over the last 7 to 10 years (to the year 2009 – when NCRP 160 was published). Two of the major advances in CT imaging that have led to this rapid growth are helical CT, which enables faster acquisition of a volume data set, and multi-detector CT (MDCT) which allows for the acquisition of a large number of thin slices during a single rotation of the x-ray tube around the patient and also has the ability to scan the entire body in less than 30 seconds (*3*).

Figure 1-1 (adapted from Figure 4.1in NCRP 160, pg. 91) illustrates the increase in CT procedures per year, from 1993 to 2006, in the United States. NCRP 160 reports an average increase of ~ 10 to 11% per year during those years and that the use of CT technology in the U.S. is likely to continue to increase over the next 10 years. For more details on the trends observed, averages obtained, and databases used to obtain such results, the reader is referred to NCRP Report No. 160.

In an article published by Brenner et al (4), the authors mention that these advances in CT imaging have had a particular effect in pediatric CT examinations; an effect particularly marked in the United States. Even though CT imaging of children represents a comparatively small fraction of the overall number of CT examinations, the authors report that there has been an increased frequency of pediatric CT, which is largely caused by the "arrival" of helical CT. The article reports an increase of 92%, between 1996 and 1999, in abdominal and pelvic CT

examinations on children less than 15 years old and an increase of 63% in requests for pediatric CT between 1991 and 1994.

The main goal of this was to assess the lifetime cancer mortality risks attributable to radiation from pediatric CT. It presented as a main result that "The larger doses and increased lifetime radiation risks in children produce a sharp increase, relative to adults, in estimated risk from CT." (*4*) The authors conclude that "The best available risk estimates suggest that pediatric CT will result in significantly increased lifetime radiation risk over adult CT." (*4*) The authors attribute these results to the fact that most facilities employing CT imaging do not adjust technique factors to take into account patient size. The article reports that several other authors have suggested that pediatric CT exposures could be reduced by 30-50% or more, relative to adult exposures, to obtain basically the same diagnostic information if patient size was taken into account (*4*).

Conventional Radiography and Fluoroscopy

These procedures now comprise the largest number of x-ray examinations performed on patients in the U.S. NCRP 160 defines conventional radiography as the use of x-ray imaging systems such as those using screen-film image receptors, computed radiography, digital radiography, direct exposure x-ray film (as used in intraoral radiography), or other types of system producing two-dimensional x-ray projection images; conventional fluoroscopy is defined as real-time projection imaging used for diagnostic purposes. Even though these procedures are currently the largest contributors to x-ray examinations, their collective effective dose is now only a relatively small portion of the total medical dose in the United States (3). Collective effective dose is the product of average-per-patient effective dose (defined in Chapter 2) and the number of patients exposed.

Out of the different modalities employed, conventional radiography, digital radiography, including computed radiography, are rapidly growing and becoming the more accepted methods for diagnostic imaging. Just as with CT, one the main reasons for their growing acceptance is time. Digital radiography offers the ability to bypass chemical processing (required with x-ray film), making the results available faster; furthermore, it offers the advantage of enhancing the images after exposure, potentially eliminating the need for re-exposure if the image does not look as desired. These images are also available for digital transfer, which again results in quicker diagnostic times and staff convenience.

NCRP 160 reports that as of 2009, it was the higher-volume facilities that were making the transition to digital radiography most rapidly, but in the future, it is expected that the number of facilities employing digital systems will increase (*3*).

Even though the use of digital radiography has increased over the last decade, its impact on the collective effective dose to the population is expected to be relatively minor. From data analyzed in NCRP 160, for 2002 to 2006, the report indicates an increase in the entrance skin exposure of 67% for a PA (posterior-anterior) chest projection and 28% for an AP (anterior-posterior) lumbar spine projection for digital imaging when compared with screen-film imaging; however, they emphasize that it is not clear that these increases in entrance skin exposure to patients are necessary and assert that with experience, the proper adjustment of technical factors may result in equivalent or even lower entrance skin exposures per examination for digital imaging compared with screen-film imaging (*3*).

Interventional Fluoroscopy

NCRP 160 defines interventional fluoroscopy as any procedure in which the use or application of a medical device is fluoroscopically guided in the body, and includes procedures that are performed for diagnostic and therapeutic purposes (*3*).

The past two decades have witnessed a major increase in high-dose fluoroscopically guided interventional procedures in medicine (*1*). Interventional fluoroscopy utilizes ionizing radiation to guide small instruments (e.g. catheters) through blood vessels or other pathways in the body. This procedure has found wide acceptance over the past decades, over invasive surgical procedures, because it only requires a very small incision therefore reducing the risk of infection during the procedure; also, due to its less invasive nature, it allows for faster recovery time when compared to surgical procedures.

Just as discussed with the previous imaging modalities, every technology has pros and cons. With the growing use of this procedure have also come public health concerns due to the increasing radiation exposure to patients and the personnel in charge of conducting the examinations. "Because of the high skin doses that can be generated in the course of these interventions, some procedures have resulted in early or late skin reactions, including necrosis in some cases. In all cases of skin reactions, the doses are thought to have been high, and the severity of some reactions has required skin grafts . . . ." (*1*)

In view of the concerns raised by reports of adverse biological effects, attempts have been made to measure and document doses resulting from procedures such as diagnostic and interventional cardiac catheterization procedures. However, to put things in perspective, considering the hundreds of thousands of patients involved each year in the United States, the problems encountered in cardiac and neurologic intervention are exceedingly rare but there is always the potential that they will occur (*1*).

It is important to note that most patients undergoing interventional fluoroscopy procedures are suffering from life-threatening conditions. In other words they are likely to die unless

something is done; therefore, when weighting the risk-benefit balance, it will be heavily influenced by the immediate benefit that could be achieved (*1*).

Nuclear Medicine

As defined by NCRP 160, nuclear medicine is the medical specialty in which unsealed radionuclides are used for diagnosis and treatment. Although nuclear medicine may be used in therapeutic procedures, it is mostly used in diagnostic examinations. Nuclear medicine images are better for examinations of physiologic and metabolic mechanisms (when compared to radiography); however, they have less spatial or anatomic resolution than do radiographic examinations. Nuclear medicine is widely used to assess blood flow, pulmonary ventilation, organ function, cellular metabolism, and other in vivo biologic processes (*3*).

Nuclear medicine was a late starter when compared with radiation therapy and x-ray diagnostics. It was not until 1946 that radiopharmaceuticals of adequate quality and consistency were available (*1*). Since then, however, nuclear medicine grew rapidly until it was somewhat slowed down by the arrival of CT and MRI (Magnetic Resonance Imaging); regardless, it continues to grow steadily and it is now an entire field of diagnostic imaging in its own. There has been ongoing development of instrumentation, new radiopharmaceuticals, and competition with other imaging techniques. Radiopharmaceuticals are usually administered by inhalation, orally, or most commonly by injection; these then localize in various target organs and tissues in the body (*3*).

Two basic modalities have evolved that characterize nuclear medicine: single-photon emission computed tomography (SPECT) and positron emission tomography (PET). SPECT utilizes conventional γ-emission from radiopharmaceuticals and is utilized in combination with planar imaging. PET is based on the simultaneous emission of a pair of photons (511 keV each) as a result of positron annihilation and it uses mostly short-lived radionuclides.

Just as with any medical exposure to ionizing radiation from different procedures, nuclear medicine carries a small increase of risk of the patient developing cancer in the future, so as with any other imaging modality, the potential risk should be weighed against the apparent benefit. This is perfectly illustrated by a recently published article (December 2011) by Dr. George Sgouros et al. (*5*), which analyzes an approach for balancing diagnostic imaging quality with cancer risk in pediatric patients. The article reported that "A recent survey of pediatric hospitals showed a large variability in the activity administered for diagnostic nuclear medicine imaging of children. Imaging guidelines, especially for pediatric patients, must balance the risks associated with radiation exposure with the need to obtain the high-quality images necessary to derive the benefits of an accurate clinical diagnosis." The authors assert that the goal of every nuclear medicine study "is to obtain the maximum diagnostic information as cost-effectively and in as short a period of time as possible and with the lowest patient radiation exposure." Furthermore, they emphasized the importance of applying these considerations to pediatric nuclear imaging by stating that "Children are generally more sensitive to radiation and have their entire lifetimes to manifest radiation effects. . . ." (*5*)

The Need for Quantifying Stochastic Risks in Medical Imaging

It is extremely vital to analyze risks to patients resulting from medical diagnostic and interventional procedures because, according to NCRP 160, such procedures contribute significantly to the collective effective dose to the U.S. population (*3*). Diagnostic imaging technology has been positively accepted in the medical community due to the services it is able to provide; however, due to this increased acceptance, it is imperative that the radiogenic risks of cancer, resulting from a technology that is being more frequently used, are analyzed.

Another reason to quantify stochastic risks in medical imaging is that, as mentioned earlier, radiation doses employed in diagnostic imaging procedures, excluding doses resulting from

accidents or interventional procedures, typically do not reach or overcome a threshold that would make the risks from the procedure deterministic in nature; the potential harmful effects of diagnostic imaging are thus stochastic in nature.

Based on the previous statement and the fact that radiation doses received by patients in interventional radiology are much higher than from general diagnostic radiology, so much that there is risk of deterministic effects, one may ask why then were interventional procedures mentioned? It is necessary to note that the possible presence of deterministic effects does not translate into the absence of stochastic effects; because the probability of stochastic effects increases with radiation dose, then the risk of occurrence for such effects is greater in interventional procedures than for diagnostic imaging because the doses are much higher. It is thus important to be able to quantify stochastic risks from interventional procedures (such as interventional fluoroscopy).

Risk quantification is a tool that can be used collectively in optimizing values of exposure, or administered activity, and resulting organ absorbed doses, to perhaps minimize the risk of radiation-induced cancer while still obtaining good quality images.

General Aims

In 2005, the BEIR (Biological Effects of Ionizing Radiation) VII Committee of the U.S. National Academy of Sciences published models for estimating risks of cancer incidence and mortality following exposure to low-LET (Linear Energy Transfer) radiation. These models take into account the subject's sex, age at exposure, dose rate and other factors. In that report, estimates for lifetime attributable risks (LAR) are given for all solid cancers, leukemia, and specific solid cancer sites. The Committee used excess relative risk (ERR) and excess absolute risk (EAR) models to project radiogenic cancer risks that are unique to the U.S. population. For most cancer sites, the Environmental Protection Agency (EPA) uses BEIR VII models for

calculating lifetime attributable risks, but with some modifications and extensions. The latter include models for calculating risks for high-LET radiation exposures and the inclusion of additional cancer sites not considered in the BEIR VII report.

In this thesis, the BEIR VII models are first presented in brief form, followed by revised EPA risk models. Differences between the BEIR VII and EPA models are presented. The research of this thesis explores the applicability of EPA models to the assessment of cancer risk resulting from medical exposures of individual patients. The EPA models have been implemented for the purpose of providing age and gender dependent LAR tables needed to better quantify stochastic risk in medical imaging studies such as nuclear medicine, fluoroscopy, and computed tomography. This approach to risk quantification is then contrasted to the use of the International Commission on Radiological Protection's (ICRP) effective dose, a quantity with limited application to medical radiation exposure, via an FDG PET/CT medical imaging simulation example. The LAR results for both methods are then analyzed and compared.

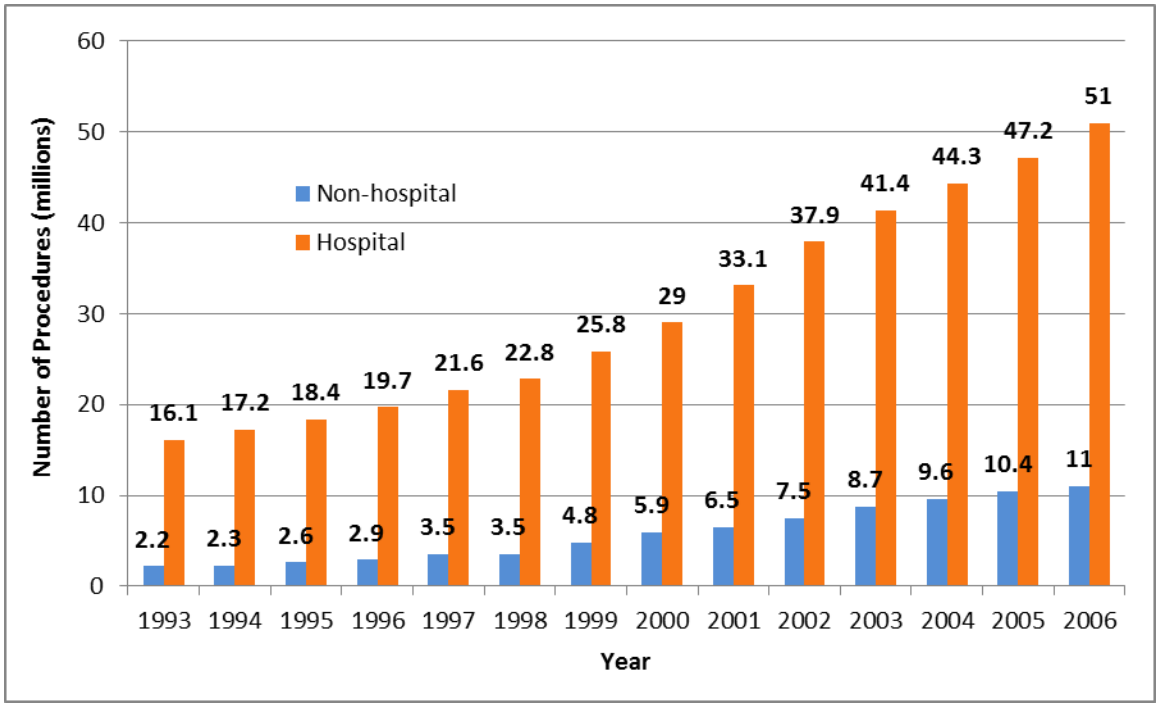

Figure 1-1. Number of CT procedures per year in the United States (millions), 1993 to 2006. Average growth: >10% y–1. (Figure adapted from Figure 4.1 in NCRP 160 – Pg. 91) (*10*)

CHAPTER 2
HISTORY AND DEVELOPMENT OF THE EFFECTIVE DOSE

Currently, effective dose (E) is the only dose quantity that is related to health detriment for stochastic effects from ionizing radiation exposures. However, *E* is a quantity with limited application to medical radiation exposure and before discussing the reasons behind this declaration, it is important to be acquainted with how this quantity originated and how it has evolved over time.

International Commission on Radiological Protection Publication 26

In 1977 the International Commission on Radiological Protection (ICRP) introduced the quantity dose equivalent (H) in Publication 26. The Commission expressed that the quantity absorbed dose (D) – the energy imparted per unit mass by ionizing radiation to matter at a specific point with units of joule per kilogram and given the special name gray (Gy) (*1*) – was not sufficient, by itself, to predict either the severity or probability of the deleterious effects on health resulting from exposure to ionizing radiation. Their intention in developing *H* was to provide a quantity that correlated better with the more important deleterious effects of exposure to radiation, more particularly with delayed stochastic effects. ICRP 26 then defined *H* as the absorbed dose, at a point in tissue, weighted by the modifying factors Q and N (*6*):

$$H = DQN. \tag{2-1}$$

In Equation 2-1, Q is a quality factor for a specific radiation type defined as a function of linear energy transfer (LET). Multiplying D by Q allows H to express, on a common scale for all ionizing radiation, the biological damage to an exposed individual, since some types of radiation are more biologically damaging internally than others (*7*). For more information on the derivation of Q and its typical values, the reader is referred to ICRP Publication 26. N is the product of all other modifying factors (e.g. absorbed dose rate and fractionation) specified by the

Commission at the location of interest. At the time of publication of ICRP 26, the Commission assigned the value 1 to N. The unit of the dose equivalent is the also the joule per kilogram, but given as the special named unit the sievert (Sv).

The Commission specified that the dose limitation for stochastic effects should be based on the sum of the weighted dose equivalents to individual tissues of the body by applying a set of tissue-weighting factors (w_T), displayed on Table 2-1 and explained below. Furthermore, ICRP stated that the annual limit for stochastic effects was to be applied to the sum of the external and internal exposures (*6*).

International Commission on Radiological Protection Publication 30

In 1979, ICRP provided an update, in Publication 30, to the dosimetry field with a new quantity called the effective dose equivalent (H_E). H_E was defined as the summation of dose equivalents to individual tissues or organs, modified by the weighting factors (w_T) first introduced in Publication 26. The weighting factors account for the varying radiation sensitivity of tissues to the induction of stochastic effects and can be thought of as relative risks or the proportion of the total stochastic risk resulting from a specific tissue, when the whole body is irradiated uniformly (*6,8*). The purpose of this new quantity was explained by ICRP when it stated that "For stochastic effects the Commission's recommended dose limitation is based on the principle that the risk should be equal whether the whole body is irradiated uniformly or whether there is non-uniform irradiation." (*6*)

For example, if various tissues or organs received a dose equivalent (H_T) under conditions of non-uniform radiation (e.g. internal exposure following ingestion of an organ-seeking radionuclide, or external partial body exposures), then H_E would represent the hypothetical uniform, whole-body dose equivalent which, if delivered to the individual, would result in the

same total risk of cancer or genetic damage (*9*). Effective dose equivalent is represented by the following equation:

$$H_E = \sum_T (w_T H_T) \quad (2\text{-}2)$$

where the subscript T indicates a specific tissue or organ. The unit for the effective dose equivalent is also the joule per kilogram, but expressed via the special named unit the sievert (Sv). Note that both the dose equivalent and the effective dose equivalent both have units of Sv, and thus one must clearly state the quantity being reported, and not give only its value in Sv.

Table 2-1 (taken from ICRP 26, paragraph 105, pg. 21) provides the values suggested by ICRP for the weighting factors. The w_T value given to the remainder tissues (0.30) is provided further clarification from the Commission; it recommended a value of $w_T = 0.06$ to be applicable to each of the five organs or tissues of the remainder receiving the highest dose equivalents, and that the exposure of all other remaining tissues can be neglected (*6*).

The selection criteria for the tissues considered by the Commission were the radiosensitivity of the organ, how essential the organ is to the well-being of the individual, and the degree to which the damage can be treated. Radiation risks were based upon the estimated likelihood of inducing a fatal malignant disease, deterministic changes, and substantial genetic defects in liveborn descendants (*9*).

International Commission on Radiological Protection Publication 60

In 1990, the ICRP, based on a reevaluation of data on radiation risks and dosimetry generated by the Radiation Effects Research Foundation, recommended new dosimetry quantities in Publication 60 (*9*). These quantities included the average-absorbed dose ($D_{T,R}$) in units of Gy, and the equivalent dose (H_T) in units of Sv.

$D_{T,R}$ changed the definition of absorbed dose to no longer be dose at a point in tissue, but averaged across the entire volume of a tissue or organ. H_T was defined as $D_{T,R}$ multiplied by a radiation weighting factor (w_R) defined strictly for the type and energy of the radiation R incident on the body or emitted by a source if within the body (basically equivalent to the former average quality factor used in ICRP 26) (*9, 10*); radiation weighting factors are independent of the tissue or organ irradiated. It is essential to note that the weighted absorbed dose is strictly a dose. The Commission explained that the change of name served to indicate the change from quality factor to radiation weighting factor (*10*). The equivalent dose in tissue T is thus given by the following equation:

$$H_T = \sum_R (w_R \, D_{T,R}). \quad (2\text{-}3)$$

Since the radiations of interest analyzed on this document are photons and electrons, for which w_R equals 1 for all energies, values for w_R are not presented. If one is interested in their values, the reader is referred to Table 1 of ICRP Publication 60 (pg. 6).

Another major update to dosimetry introduced in ICRP 60 was the concept of effective dose (E). The weighted equivalent dose was previously called effective dose equivalent in ICRP 30; however, in Publication 60, the Commission decided that the name was "unnecessarily cumbersome" and determined to use the simpler name effective dose. Its introduction was associated with the change to equivalent dose (*10*).

Effective dose is defined as the sum of the weighted equivalent doses in all tissues and organs of the body and given by

$$E = \sum_T (w_T \, H_T) \quad (2\text{-}4)$$

where H_T is the equivalent dose in tissue (or organ) T and w_T is the tissue weighting factor for that tissue, which represents the relative contribution of that organ or tissue to the total detriment

due to the stochastic effects resulting from uniform-whole body irradiation. The Commission chose the tissue weighting factors to be independent of the type and energy of the radiation incident on the body (*10*). "It is desirable that a uniform equivalent dose over the whole body should give an effective dose numerically equal to that uniform equivalent dose. This is achieved by normalising the sum of the tissue weighting factors to unity." (*10*) Table 2-2 (Table 2 of ICRP 60, pg. 8) displays the new tissue weighting factors defined by ICRP 60.

ICRP 60 made the following disclaimer about the newly introduced quantities: "Both equivalent dose and effective dose are quantities intended for use in radiological protection, including the assessment of risks in general terms. They provide a basis for estimating the probability of stochastic effects only for absorbed doses well below the thresholds for deterministic effects. For the estimation of the likely consequences of an exposure of a known population, it will sometimes be better to use absorbed dose and specific data relating to the relative biological effectiveness of the radiations concerned and the probability coefficients relating to the exposed population." (*10*)

International Commission on Radiological Protection Publication 103

In 2007 ICRP made updates to the quantities equivalent and effective dose in Publication 103. The use of the quantities remained unchanged; the revisions were made to the methods used in their calculations (*11*). Equivalent dose is still defined in this publication as in Equation 2-3 and effective dose as per equation 2-4 and both quantities are still expressed in units of Sv under this publication.

Review of available data, together with biophysical considerations, led the Commission to make changes to the radiation weighting factors used for neutrons and protons, with values for neutrons given as a continuous function of neutron energy, and the inclusion of a value for charged pions. Radiation weighting factors, w_R, for the other radiation types remained

unchanged (*11*). As mentioned in the previous section, since the radiation of interest analyzed in this document are photons and electrons, for which w_R still equals 1 for all energies under ICRP 103, values for w_R are not presented. The reader is referred to Table 2 of ICRP Publication 103 (pg. 64). Furthermore, due to availability of new epidemiological data on cancer induction, some of the tissue weighting factors, w_T, were changed under Publication 103 (Table 2-3). Aside from the sex- and age-averaging, the steps involved in the development of the tissue weighting system employed by ICRP 103 are more complex and include various stochastic endpoints such as cancer mortality, cancer morbidity, and years of life lost. For more details on the development of this system, the reader is referred to page 191 of ICRP Publication 103.

It is very important to mention a change made by ICRP to the calculation methodology of doses from external and internal sources. As specified in Publication 103, these doses will be calculated using reference computational phantoms of the human body based on tomographic images, replacing the previous use of mathematical models. "For adults, equivalent doses will be calculated by sex-averaging of values obtained using male and female phantoms. Effective dose will then be calculated using revised age- and sex-averaged tissue weighting factors, based on updated risk data and intended to apply as rounded values to a population of both sexes and all ages." (*11*) It is crucial to note that the Commission states that "Effective dose is calculated for a Reference Person and not for an individual." Refer to Figure 2-1 (Figure 2 of ICRP 103, pg. 68) for an illustration of this procedure.

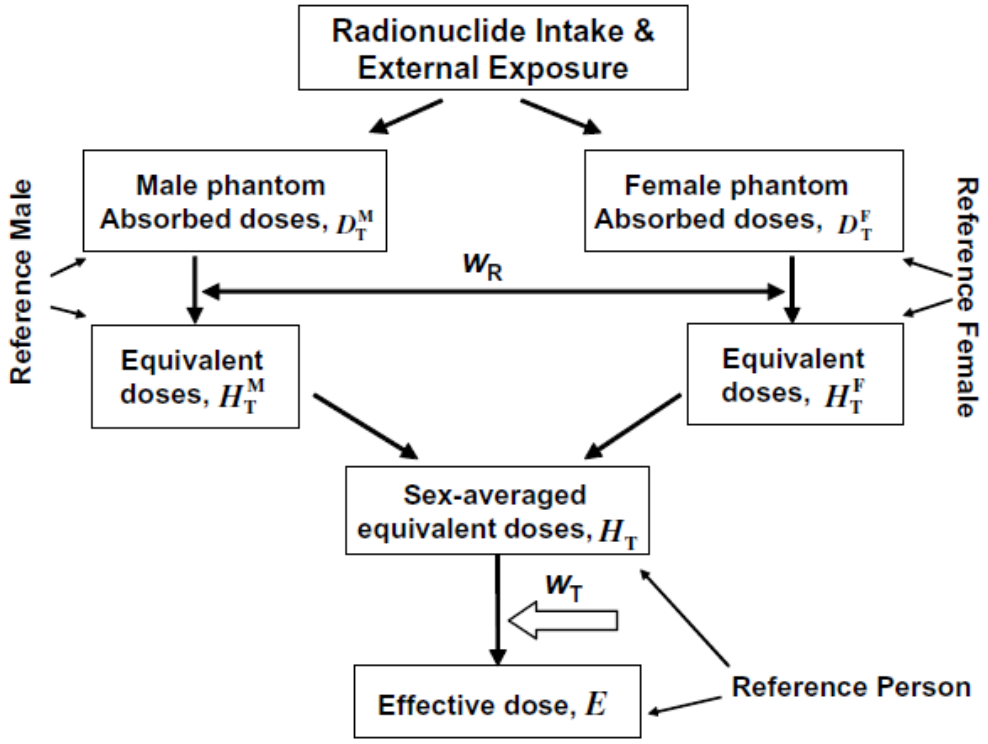

Figure 2-1. ICRP 103 steps in calculating effective dose (Figure 2 of ICRP 103, pg. 68) (*11*)

Table 2-1. IRCP 26 weighting factors (w_T) for calculating effective dose equivalent (H_E)

Tissue	w_T
Gonads	0.25
Breast	0.15
Red bone marrow	0.12
Lung	0.12
Thyroid	0.03
Bone surfaces	0.03
Remainder	0.3

Notes:

* $w_T = 0.06$ applied to the five remaining tissues receiving the highest dose equivalent (H_T); all other tissues are neglected

*Table taken from ICRP 26, Pg. 21 (*6*)

Table 2-2. ICR[60 tissue weighting factors[1] (w_T) for calculating effective dose (E)

Tissue or organ	Tissue weighting factor, w_T
Gonads	0.20
Bone marrow (red)	0.12
Colon	0.12
Lung	0.12
Stomach	0.12
Bladder	0.05
Breast	0.05
Liver	0.05
Esophagus	0.05
Thyroid	0.05
Skin	0.01
Bone surface	0.01
Remainder	0.05[2, 3]

Note: Table taken from ICRP 60, pg. 8 (*10*)

[1] The values have been developed from a reference population of equal numbers of both sexes and a wide range of ages. In the definition of effective dose they apply to workers, to the whole population, and to either sex.

[2] For purposes of calculation, the remainder is composed of the following additional tissues and organs: adrenals, brain, upper large intestine, small intestine, kidney, muscle, pancreas, spleen, thymus and uterus. The list includes organs which are likely to be selectively irradiated. Some organs in the list are known to be susceptible to cancer induction. If other tissues and organs subsequently become identified as having a significant risk of induced cancer they will then be included either with a specific w_T or in this additional list constituting the remainder. The latter may also include other tissues or organs selectively irradiated.

[3] In those exceptional cases in which a single one of the remainder tissues or organs receives an equivalent dose in excess of the highest dose in any of the twelve organs for which a weighting factor is specified, a weighting factor of 0.025 should be applied to that tissue or organ and a weighting factor of 0.025 to the average dose in the rest of the remainder as defined above.

Table 2-3. ICRP 103 tissue weighting factors (w_T) for calculating effective dose (E)

Tissue	w_T	$\sum w_T$
Bone-marrow (red), Colon, Lung, Stomach, Breast, Remainder tissues*	0.12	0.72
Gonads	0.08	0.08
Bladder, esophagus, Liver, Thyroid	0.04	0.16
Bone surface, Brain, Salivary glands, Skin	0.01	0.04
	Total	1

Note: Table 3 in ICRP 103, pg. 65 (*11*)

* Remainder tissues: Adrenals, Extrathoracic (ET) region, Gall bladder, Heart, Kidneys, Lymphatic nodes, Muscle, Oral mucosa, Pancreas, Prostate (♂), Small intestine, Spleen, Thymus, Uterus/cervix (♀).

CHAPTER 3
USE AND MISUSE OF THE EFFECTIVE DOSE IN MEDICINE

Principles of Radiological Protection (International Commission on Radiological Protection)

A good starting point for understanding ICRP's sanctioned proper use of the effective dose in medicine is to analyze the principles of radiological protection given by the Commission. In its 1990 Recommendations (ICRP Publication 60), the Commission gave principles of protection separately from intervention situations. In the 2007 Recommendations (ICRP Publication103), the Commission continued to consider these principles as essential for the system of protection, and formulated a single set of principles that apply to planned, emergency, and existing exposure situations. These principles are known as justification, optimization of protection, and application of dose limits. Justification and optimization are regarded as source-related and apply in all exposure situations; the application of dose limits is individual-related and applies in planned exposure situations, except medical exposure of patients (*11, 12*). The Commission states that "Provided that the medical exposures of patients have been properly justified and that the associated doses are commensurate with the medical purpose, it is not appropriate to apply dose limits or dose constraints to the medical exposure of patients, because such limits or constraints would often do more harm than good." (*11*)

The previous paragraph binds effective dose to be used only for justification and optimization in medical exposures since limitation does not apply. Since the medical example considered in this document (FDG PET/CT simulation) is regarded as a planned medical exposure, the principle of limitation is not further analyzed; for more details on this principle, the reader is referred to ICRP Publications 103 and 105.

Based on the principle of justification, any decision that "alters the radiation exposure situation should do more good than harm. This means that, by introducing a new radiation

source, by reducing existing exposure, or by reducing the risk of potential exposure, one should achieve sufficient individual or societal benefit to offset the detriment it causes." (*11*) However, medical exposure of patients calls for a more detailed approach to the process of justification (refer to ICRP 105) that goes beyond the scope of this document, although the main idea just defined still applies; the Commission only recommends that "justification require that net benefit be positive." (*11*)

Based on the principle of optimization, the likelihood of "incurring exposures, the number of people exposed, and the magnitude of their individual doses should all be kept as low as reasonably achievable, taking into account economic and societal factors." (*11*) What the Commission means by this is that "the level of protection should be the best under the prevailing circumstances, maximising the margin of benefit over harm. In order to avoid severely inequitable outcomes of this optimisation procedure, there should be restrictions on the doses or risks to individuals from a particular source (dose or risk constraints and reference levels)." (*11*)

Applications of Effective Dose to Medical Dosimetry

In Publication 103, ICRP advises how effective doses should be applied to medical exposures and extends these recommendations in its Publication 105. First, it is extremely important to note that ICRP intended effective dose for use as a principal protection quantity for the establishment of protection guidance in radiology. ICRP states that "It should not be used to assess risks of stochastic effects in retrospective situations for exposures in identified individuals, nor should it be used in epidemiological evaluations of human exposure. . . ." (*12*) The risks for such stochastic effects are age and sex dependent and this has definite implications.

The Commission derived the effective dose for age and sex distributions of workers and the general population, which can be very different from the overall age and sex distribution for patients undergoing specific medical procedures that utilize ionizing radiation; moreover, these

distributions will vary from one medical procedure to another, since the medical condition being evaluated under such procedures may vary and so will the prevalence of individuals undergoing the different procedures (*11, 12*). "For these reasons, risk assessment for medical diagnosis and treatment using ionising radiation is best evaluated using appropriate risk values for the individual tissues at risk and for the age and sex distribution of the individuals undergoing the medical procedures." (*11, 12*)

As explicitly mentioned by ICRP, effective dose can be of practical importance for comparing the relative doses related to stochastic effects from the following scenarios: different diagnostic examinations and interventional procedures, the use of similar technologies and procedures in different hospitals and countries, and the use of different technologies for the same medical examination provided that the representative patients or patient populations for which the effective doses are derived are similar with regard to age and sex (*11, 12*). In many cases, this last condition is clearly not met. For example, any medical procedure used only in children will negate the averaging of radiation detriments across all ages, as is done in establishing the ICRP values of its tissue weighting factors.

Reference Conditions

As mentioned at the end of Chapter 2, one of the more important updates to the effective dose made by ICRP, in its Publication 103, was the explicit use of reference computational phantoms of the human body (obtained from tomographic images), replacing the previous use of stylized or mathematical models.

Note the following definitions taken from ICRP 103, pg. 31, which are of importance for the understanding of the reference conditions:

- Reference Male and Reference Female (Reference Individual) – An idealized male or female with characteristics defined by the Commission for the purpose of radiological protection,

and with the anatomical and physiological characteristics defined in the report of the ICRP Task Group on Reference Man – Publication 89 (*13*).

- Reference Person – An idealized person for whom the organ or tissue equivalent doses are calculated by averaging the corresponding doses of the Reference Male and Reference Female. The equivalent doses of the Reference Person are used for the calculation of the effective dose by multiplying these doses by the corresponding tissue weighting factors.
- Reference phantom – Voxel phantoms for the human body (male and female voxel phantoms based on medical imaging data) with the anatomical and physiological characteristics defined in the report of the ICRP Task Group on Reference Man – Publication 89 (*13*).

Consistent with the approach taken in Publication 23 (*14*), the ICRP reiterates in Publication 89 that "it is neither feasible nor necessary to specify a reference individual as being representative of a well-defined population group. To construct a useful reference individual, it is important to have a full set of consistent results so that the sum of the parts adds up to a proper value for the total body." (*13*) For this reason, and since data on these populations had been well studied (anatomically and physiologically), the Commission chose to use data on Western Europeans and North Americans as the basis for defining ICRP reference values (*13*).

In Publication 89, ICRP states that in order to calculate radiation dose to the human body (from external or internal sources), information about the anatomy and physiology of the exposed individual is required, and that this information is particularly needed when calculating doses from internally deposited radionuclides to various organs and tissues in the body. However, since the characteristics of an exposed person vary from one individual to another, the Commission deemed important to have a set of reference values to describe various anatomical and physiological attributes of an exposed individual; this allows for consistent and reproducible

radiation protection guidance for different types of exposure. “An important attribute is that these reference values for tissues and organs, when summed, define a reference individual. Consideration of an entire reference individual helps to ensure that there will be an internal consistency about how the volume, mass or functional characteristics of various organs or tissues are specified.” (*13*)

ICRP Committee 3 (C3) Task Group developed reference biokinetic models (useful in nuclear medicine) that model the different pathways different radiopharmaceuticals may take when in the body.

Reference values are derived for radiation protection purposes for adult workers (male and female) and members of the general public. Reference values for the size and composition of organs, as well as reference physiological information, provide the main design criteria for models (referred to as reference phantoms) of the reference individual features. Reference values for anatomical features refer to, for example, overall height, weight, length of extremities, etc. Physiological information refers to, metabolic, excretion, respiration, and energy expenditure rates, just to mention a few. For more information and actual values of these reference conditions, the reader is referred to ICRP Publication 89 (*13*).

Misuse of the Effective Dose

As mentioned in Chapter 2, and stated in ICRP Publication 103, effective dose is derived using the average of the equivalent doses for Reference Male and Reference Female and applying to that average tissue weighting factors which are sex- and age- averaged; effective dose is therefore calculated for a Reference Person and not for a specific individual, as intended by ICRP. This definition of effective dose results in several implications and limitations to the quantity, when it comes to medical exposures to ionizing radiation, which makes it prone to being easily misused.

An example of misuse could be seen in cases such as CT or fluoroscopically guided interventional procedures, in which the exposure conditions may be patient-specific; however, if one is truly calculating an ICRP value of effective dose, then the exposure conditions cannot be patient-specific, they must be reference patient or person (both male and female) since effective dose was defined under those conditions.

When the anatomic model is non-reference in any way, such as the use of underweight or overweight computational phantoms for use on specific circumstances, then the quantity reported is technically no longer an effective dose. Another scenario under which reporting dose as effective dose is erroneous is when the biokinetic model for nuclear medicine dosimetry is based upon-patient specific imaging data, and not the standardize biokinetic models developed by the C3 Task Group. In other words, if the exposed individual deviates in any way (anatomical, physiological, or biokinetics) from the reference conditions needed to calculate effective dose, then the quantity reported is no longer a value of effective dose as technically defined by ICRP.

Again, it is important to note that ICRP reference dose coefficients are not aimed at providing a dose for a specific individual but for a Reference Person (*11*). Furthermore, ICRP clearly states that effective dose is not to be used for detailed specific retrospective investigations of individual exposure and risk (*11*). However, some people still want to report the effective dose and assign it to individual patients, disregarding ICRP recommendations. Effective dose never belongs to an individual patient, just as the effective dose never belongs to an individual worker or member of the general public. The quantity only belongs to the reference person or reference patient.

In order to analyze the risk (of cancer incidence or mortality) from medical imaging procedures utilizing the effective dose, the quantity must be corrected using a detriment adjusted

nominal risk coefficient, obtained from cancer incidence data, which is reported in ICRP 103 as 5.5×10^{-2} Sv^{-1}; the Commission states as its policy that the nominal risk coefficients do not apply to individuals but rather should be applied to whole populations (*11*). Some people then report the product of effective dose and the nominal risk coefficient as a risk of cancer incidence to an individual even though the risk coefficients were not designed for individuals. Furthermore, it must be noted that when these two quantities are multiplied, the resulting value is considered an effective-dose derived overall risk for "radiation detriment", which includes cancer incidence but is not solely a risk of cancer incidence; radiation detriment is defined in ICRP Publication 60 (*10*) and Publication 103 (*11*), and includes various stochastic endpoints such as cancer mortality, cancer morbidity, and years of life lost. The use of the term "radiation detriment" was intentionally introduced by ICRP to clarify that other subjective judgments have been applied in the establishment of w_T values, other than fundamental values of cancer incidence or mortality.

As mentioned earlier, "risk assessment for medical diagnosis and treatment using ionising radiation is best evaluated using appropriate risk values for the individual tissues at risk and for the age and sex distribution of the individuals undergoing the medical procedures." (*11, 12*)

It is important to note that it is virtually impossible to report "true" individual risks of stochastic effects because every person is completely different from one another and the variables that can change from one individual to the next are practically infinite (anatomical and physiological) making it infeasible to account for all such changes. However, based on the previous discussion, it is evident that the medical community is in need of some indicator of stochastic risk for justification and/or optimization of medical procedures, involving ionizing radiation, that at the very least takes into account variations with age and sex.

CHAPTER 4
ALTERNATIVES TO THE EFFECTIVE DOSE

As mentioned at the end of Chapter 3, there is a growing need of some indicator of stochastic risk, for justification and/or optimization of medical procedures involving ionizing radiation that at least takes into account variations in age and sex. In 2008, David Brenner proposed an alternative to the effective dose-derived risk of radiation detriment that has the potential to allow for dependencies on sex and age when assessing risks of stochastic effects.

In his article, Effective dose: a flawed concept that could and should be replaced (*2*), Dr. Brenner proposes the introduction of a new quantity called effective risk (R), defined as:

$$R = \sum_T (r_T H_T) \tag{4-1}$$

where R represents the summation across all tissues, T, of the product between organ-specific radiation-induced cancer risks (r_T) and equivalent dose (H_T) The effective risk would then be a lifetime radiation-attributable cancer risk. Equivalent dose would be calculated just as in ICRP Publication 103; the main and major difference arises with the introduction of r_T. This new factor represents the lifetime radiation-attributable tissue-specific cancer risks (per unit equivalent dose to tissue T); the effective risk would then be a lifetime radiation-attributable risk of cancer incidence resulting from various equivalent doses to the exposed tissues T(*2*).

Dr. Brenner refers to *R* as a more "simple, less confusing, easy-to-estimate quantity, based on defensible science, which more directly does the job of comparing the risks associated with different inhomogeneous doses" than the currently used "flawed concept" of effective dose.

He presents as arguments against the effective dose the fact that tissue weighting factors "represent a committee-determined subjective balance between the different stochastic endpoints of cancer incidence, cancer mortality, life shortening and hereditary risk" and that improvement in the derivation of their newer values is not so much due to an improvement in "our knowledge

of radiation risks" but rather the fact that "different groups of experts will naturally have somewhat differing views on the relative importance of the different endpoints that comprise the radiation induced 'detriment'." Furthermore he states that effective dose is "defined to be independent of age at exposure, whereas data suggest that attributable radiation risks are often highly age-dependent, and that risks for different endpoints have different age at-exposure dependencies." Finally he presents a third major problem with the concept of effective dose which he defines as a more "practical one" and is that it is often "confused and misused" due to the same units, sieverts, in which equivalent dose and effective dose are reported, even though they represent completely different quantities (*2*)

In June 2011, Dr. Xiang Li et al. published an article titled Patient-specific Radiation Dose and Cancer Risk for Pediatric Chest C*T* (*15*). The purpose of this article was to "estimate patient-specific radiation dose and cancer risk for pediatric chest computed tomography (CT) and to evaluate factors affecting dose and risk, including patient size, patient age, and scanning parameters." The authors calculated effective dose for their exposure scenarios as a comparison to their new proposed quantity risk index. The article stated that "While widely used as a surrogate for population radiation risk, effective dose does not reflect individual patient risk. . ." since it is based on the sex- and age-averaged tissue weighting factors. Therefore, "to more accurately estimate individual patient risks. . ." they "implemented a metric of risk, termed risk index. . ." which is defined as:

$$Risk\ index = \sum_T r_T\,(sex, age)\,H_{T,} \qquad (4\text{-}2)$$

where H_T is the equivalent dose for organ or tissue T and r_T is the sex-, age-, and tissue-specific risk coefficient (cases per 100000 exposed to 0.1 Gy) for lifetime attributable risk of cancer incidence obtained from the BEIR (Biological Effects of Ionizing Radiation) VII report (*16*).

The authors adopted their metric of risk index from the concept of effective risk previously proposed by Dr. Brenner. They, however, use the term risk index, as opposed to effective risk, to "reflect the inherent uncertainties associated with any risk estimation, particularly risks for individual patients, who might have different radiosensitivity due to genetic predispositions or hormonal profiles." (*15*) In both cases, risk index and effective risk, are summing the product of organ equivalent doses and lifetime attributable cancer risk incidence.

The methods previously proposed are implemented in this document for risk assessment from an FDG PET/CT medical imaging simulation example by utilization of lifetime attributable risks (LAR). It is important to note, however, that both of the methods discussed are based on cancer incidence data. "These data not only include nonfatal cancers, but also offer diagnostic information that is of higher quality than that based on death certificates, which is especially important when evaluating site-specific cancers." (*16*) While this allows for more reliable data and a wider range of coverage of individuals, since reportedly there are more cases of cancer incidence than cancer mortality (refer to the BEIR VII report), basing risk assessment solely on cancer incidence data has some disadvantages; one is that the large differences in the success rates for treatment of different cancer types would be ignored, since future developments in cancer treatment are likely to further impact the number of incidence-cases. Also, risk assessment should be made for both morbidity and mortality, so one should use both U.S. morbidity and mortality data to be able to determine what percentage of radiogenic cancers in the U.S. will be fatal. Moreover, mortality data offer the advantage of covering a longer period (1950–2000) than the incidence data (1958–1998) and of including deaths of LSS (Life Span Study) members who migrated from Hiroshima and Nagasaki to other parts of Japan (*16*). Therefore, both LAR of cancer incidence and mortality are reported on this document.

CHAPTER 5
LIFETIME ATTRIBUTABLE RISK MODELS

As mentioned in the Introduction, in 2005, the BEIR (Biological Effects of Ionizing Radiation) VII Committee published models for estimating radiogenic risks of cancer incidence and mortality following exposure to low-LET (Linear Energy Transfer) radiation. These models take into account sex, age at exposure, dose rate and other factors. For most cancer sites, the Environmental Protection Agency (EPA) uses BEIR VII models for calculating lifetime attributable risks (LAR), but with some modifications and extensions as described in the 2011 EPA Radiogenic Cancer Risk Models and Projections for the U.S. Population report, also known as the Blue Book (*17*). The LAR of a premature cancer (or cancer death) is expressed as quantity that approximates the probability an individual will develop (or die from) cancer associated with an exposure. The Blue Book includes models for calculating risks for high-LET radiation exposures and for additional cancer sites not considered in the BEIR VII report. Both organizations use excess relative risk (ERR) and excess absolute risk (EAR) project radiogenic cancer risks for the U.S. population in their LAR calculations.

The EPA models were utilized in this document for the risk assessment of an FDG PET/CT medical imaging simulation example and to provide comparison with the effective dose-derived risk of radiation detriment, presented by ICRP in Publication 103. These risk models were coded using Microsoft Office Excel 2007 (*18*).

Although the risk models used here were mainly derived from the BEIR VII report (*16*) and the Blue Book (*17*), it is important to acknowledge that there are other data sources for calculation of LAR, mainly ICRP Publication 103 (*11*) and UNSCEAR (United Nations Scientific Committee on the Effects of Atomic Radiation) reports (*19*). “For most cancer sites, UNSCEAR and ICRP ERR and EAR risk models were derived from analyses of recent A-bomb

survivor data. . . . As in BEIR VII, most ICRP models were based on 1958-1998 incidence data, whereas the UNSCEAR models were based on 1950-2000 mortality data. ICRP models were applied to a mix of Euro-American and Asian populations; the UNSCEAR models were applied to 5 populations (China, Japan, Puerto Rico, U.S., and United Kingdom)." (*17*) Since the models from ICRP and UNSCEAR are not the primary focus of this document, the reader is referred to the respective documents for more details on their model development and use.

The following is a brief description of the BEIR VII models. The models are described per major cancer site, a general methodology for calculating LARs is then presented, including updates performed by the EPA, and finally LARs based on the updated EPA models are tabulated as number of cases (or deaths) per 100,000 persons exposed to a single dose of 0.1 gray (Gy).

2005 BEIR (Biological Effects of Ionizing Radiation) VII Models

Background

These models provide the basis for sex- and age-specific estimates for exposure scenarios at various ages, which are of significant value when quantifying stochastic risk to individuals from medical imaging procedures. As mentioned earlier, these models were primarily based on incidence data. BEIR VII Committee justifies this decision by stating that incidence "data not only include nonfatal cancers, but also offer diagnostic information that is of higher quality than that based on death certificates, which is especially important when evaluating site-specific cancers." (*16*)

BEIR VII uses excess relative risk (ERR) and excess absolute risk (EAR) models to project radiogenic cancer risks that are unique to the U.S. population in their LAR calculations. As defined by the Committee, ERR represents the rate of cancer (incidence or mortality) in a population exposed to low-LET radiation divided by the cancer rate in an unexposed population

and subtracting 1 from that result. EAR is defined as the rate of cancer in an exposed population minus the rate of cancer in an unexposed population (*16*).

The Committee provided models for cancers of the stomach, colon, liver, lung, female breast, prostate, uterus, ovary, bladder, and all other solid cancers (which are operationally equivalent to the remainder tissue category given in the effective dose as defined by ICRP 103 – refer to Table 2-3 in Chapter 2). Incidence estimates were also provided for thyroid cancer.

Description of Models

Site-specific solid cancers other than breast and thyroid

Models for estimating risk of solid cancers of specific sites other than breast and thyroid are of the form:

$$ERR(e, a) \text{ or } EAR(e, a) = \beta_s D \exp(\gamma e^*) (a/60)^{\eta} \quad (5\text{-}1)$$

Here, D is the equivalent dose (in Sv) and β_s is the risk (ERR or EAR) per unit equivalent dose and is also a function of sex. The risk is modified by e, age at exposure in years, e* which is equal to (e – 30)/10 when $e < 30$, and equal to zero when $e \geq 30$, and a, attained age in years. The parameters γ and η quantify the dependence of the ERR or EAR on e and a respectively.

The Committee's preferred ERR and EAR models for site specific cancer incidence and mortality are shown in Table 5-1 (Table 12-2 in BEIR VII report, pg. 272).

Breast

Although BEIR VII calculates LAR estimates based on both the ERR and EAR models, their preferred estimates are based on the EAR model. With that model, according to the committee, "the estimated m.ain effect is more stable because it is based on both LSS and U.S. women. In addition, this model includes both age at exposure and attained age as modifying factors and is thus more comparable to models used for other sites" (*16*). The EAR model is as follows:

$$EAR(D, s, e, a) = D\,\beta \exp[\gamma (e - 25)/10)]\,(a / 50)^{\eta}, \quad (5\text{-}2)$$

where e is exposure age and a is attained age (years); $\eta = 3.5$ for $a < 50$ and $\eta = 1.1$ for $a \geq 50$.

Thyroid

BEIR VII's preferred model for estimating thyroid cancer incidence is based on a pooled analysis of data from seven thyroid cancer incidence studies (refer to the BEIR VII report for more details on such studies). The Committee's models are as follows:

$$ERR/Gy = 0.53 \exp[-0.083 (e - 30)] \text{ for males,} \quad (5\text{-}3)$$

and

$$ERR/Gy = 1.05 \exp[-0.083 (e - 30)] \text{ for females.} \quad (5\text{-}4)$$

Leukemia

The Committee's models for estimating leukemia risks were based on analyses of LSS leukemia mortality data for the period 1950–2000. Chronic lymphocytic leukemia (CLL) was excluded from the baseline rates utilized for calculations of risk of leukemia (refer to BEIR VII for analysis on this decision). The Committee's preferred models are of the following form:

$$EAR \text{ or } ERR(D, s, e, t) = \beta s\, D\,(1 + \theta D) \exp[\gamma e^{*} + \delta \log(t / 25) + \varphi e^{*} \log(t / 25)] \quad (5\text{-}5)$$

where D is the equivalent dose (Sv), s is sex, and e* is $(e - 30)/10$ for $e < 30$ and 0 for $e \geq 30$ (e is age at exposure in years). The parameter θ indicates the degree of curvature (not dependent on sex, age at exposure, or time since exposure). The parameter β_S represents the ERR/Sv or the EAR (expressed as excess deaths per 104 PY-Sv, where PY = person-years). Table 5-2 (Table 12-3 in BEIR VII report, pg. 274) contains the parameter estimates needed for the model.

For this thesis, the target tissue analyzed for LAR of leukemia (incidence or mortality) is the active bone marrow.

General Methodology for Calculating Lifetime Attributable Risks

This section contains the general methodology utilized by the BEIR VII Committee for calculating LARs of cancer incidence or mortality for site-specific solid cancers and for leukemia based on EAR estimates. EAR can be obtained by using EAR models directly or by multiplying the ERR models by a baseline rate (λ) of cancer incidence or mortality for the U.S. population (refer to the section Risks of cancer incidence below). BEIR VII calculates the LAR for a person exposed to dose *D* at age *e* as follows:

$$LAR(D, e) = \sum_a M(D, e, a)\, S(a) / S(e), \quad (5\text{-}6)$$

where the lifetime risk for a given age of exposure is the summation of risks of developing or dying from cancer at ages a = e + L to l00. Here, a is the attained age (years) and L is a risk-free latent period (5 years for solid cancers and 2 for leukemia). The M(D, e, a) is the EAR (either used directly from EAR or indirectly from ERR models), S(a) is the probability of surviving until age a, and S(a) / S(e) is the probability of surviving to age a conditional on survival to age e. The values for S(a) were obtained from a 1999 life table for the U.S. population (*20*).

Once LARs have been obtained either using EAR transport directly or ERR transport, the answers from both methods are combined to obtain an LAR as follows:

$$LAR_{COMB} = (LAR_{ERR})^{0.7}\ (LAR_{EAR})^{0.3} \quad (5\text{-}7)$$

This weighting scheme is performed for sites other than breast, thyroid, and lung. As stated in the BEIR VII report, this choice was made because there is somewhat greater support for relative risk than for absolute risk transport. For lung cancer, the weighting scheme is reversed and a weight of 0.7 is used for the EAR estimate and one of 0.3 for the ERR estimate (refer to BEIR VII for the underlying rationale). This weighting scheme is not implemented for breast cancer

risk estimates for which the LAR is based on the direct EAR model only, nor for thyroid cancer for which only the ERR model is used (*16*).

Once the answers from both transport methods (EAR and ERR) have been combined, a final total LAR can obtained as follows:

$$LAR_{TOT} = LAR_{COMB} / DDREF, \quad (5\text{-}8)$$

where the DDREF is 1.5 (used to estimate risk for solid tumors) and is the dose and dose rate effectiveness factor needed for extrapolating data from acute high-dose-rate experiments. To estimate the risks of leukemia (incidence or mortality), BEIR VII uses a linear-quadratic model and therefore does not require a DDREF adjustment (*16*).

Risks of cancer incidence

Lifetime risks estimates of cancer incidence obtained using relative risk transport were based on ERR models as follows:

$$M(D, e, a) = ERR(D, e, a)\, \lambda_I^{\,c}(a), \quad (5\text{-}9)$$

where the ERR(D, e, a) was obtained from the models shown in Tables 5-1 and 5-2. The $\lambda_I^{\,c}(a)$ represents sex- and age-specific 1995–1999 U.S. cancer incidence rates from Surveillance Epidemiology, and End Results (SEER) registries, where *c* designates the cancer site or category. Lifetime risk estimates of cancer incidence using absolute risk transport were based on EAR models as follows:

$$M(D, e, a) = EAR(D, e, a) \quad (5\text{-}10)$$

where the EAR(D, e, a) was obtained from the models shown in Tables 5-1 and 5-2 as well.

Risks of cancer mortality

Lifetime risks estimates of mortality obtained using relative risk transport were based on ERR models as follows:

$$M(D, e, a) = ERR(D, e, a)\, \lambda_M^{\,c}(a), \quad (5\text{-}11)$$

where the ERR(D, e, a) is the same model used for lifetime risk estimates of cancer incidence and was obtained from the models shown in Tables 5-1 and 5-2. However, $\lambda_M{}^c$ (a) represents sex- and age-specific 1995–1999 U.S. cancer mortality rates where c also designates the cancer site or category. Lifetime risk estimates using absolute risk transport were based on EAR models also taken from Tables 5-1 and 5-2; but to estimate site-specific cancer mortality, it was necessary to adjust the EAR(D, e, a) by multiplying by $\lambda_M{}^c$ (a) / $\lambda_I{}^c$ (a), the ratio of the sex- and age-specific mortality and incidence rates for the U.S. population. So for site-specific mortality,

$$M(D, e, a) = EAR(D, e, a)\, \lambda_M{}^c(a) / \lambda_I{}^c(a). \quad (5\text{-}12)$$

Leukemia

Models for leukemia differ from those for solid cancers in that risk is expressed as a function of age at exposure (e) and time since exposure (t) instead of age at exposure and attained age (a). Time since exposure can then be written as a – e. To obtain ERR(D, e, a) or EAR(D, e, a) one simply substitutes *a – e* for *t* in Equation 5-5. Furthermore, for the period 2–5 years after exposure, the EAR (whether used directly or from ERR models) is assumed to be the same as that at 5 years after exposure (*17*). In other words, for a = e + 2 to e + 5, M(D, e, a) = M(D, e, e + 5).

2011 Environmental Protection Agency Models

Similarities/Differences From BEIR (Biological Effects of Ionizing Radiation) VII Models

For most site-specific solid cancers (other than breast and thyroid) and leukemia, the EPA has applied the same ERR and EAR models as given in the BEIR VII Report and as described in Tables 5-1 and 5-2. However, the LAR is calculated as a sum of risks from ages *e + L* to 110, and values for S(a) were obtained from a 2000 life table (*17*)., as opposed to the 1999 life table used in BEIR VII (*16*) . EPA also used more up-to-date cancer specific incidence and mortality rates (refer to the 2011 EPA Blue Book for detailed information on such rates) (*17*).

Weighting scheme

Another major difference in the calculation process of the LAR, is the combination of LAR results obtained from ERR and EAR models. BEIR VII uses a weighted geometric mean approach to the combination of models as illustrated by Equation 5-7. EPA has instead employed a weighted arithmetic mean to combine ERR and EAR projections, which they assert "has a relatively straightforward interpretation and is additive" (*17*).

The EPA implements the following weighted arithmetic mean approach:

$$LAR^{(EPA)}(D, e) = w^* LAR^{(R)}(D,e) + (1-w^*) LAR^{(A)}(D,e) \quad (5\text{-}13)$$

where $LAR^{(A)}$ and $LAR^{(R)}$ represent the age-and-sex specific LARs derived from the EAR and ERR models, respectively. Similar to that in BEIR VII, the weight given to $LAR^{(R)}$ is 0.7 ($w^*=0.7$) and thus the one given to $LAR^{(A)}$ is 0.3 ($1-w^*=0.3$). Also as in BEIR VII, the $LAR^{(EPA)}$ is adjusted down by a DDREF of 1.5 for all cancer sites except leukemia, bone and skin. The 2011 EPA Blue Book (*17*) has a more detailed examination on the development of this weighting scheme.

Breast

EPA's methodology for calculating LAR of breast cancer incidence is identical to that used by BEIR VII. For estimates of LAR of breast cancer mortality, however, EPA uses a very different method than that employed by BEIR VII. The methodology is much more complex than the one for risk of breast cancer incidence, so for details on its development refer to Appendix A (taken from the Blue Book, pgs. 44-47).

The main reason EPA uses a different method for estimating lifetime radiogenic risks for breast cancer mortality, is because BEIR VII's methods did not take into account the often long time of survival between breast cancer diagnosis (incidence) and death (*17*). EPA's method does take this into account. For cancers such as lung and liver, for example, survival is still very short

so it is not as important to account for this period of time. For some other cancers like breast and prostate, survival times are long. It was deemed by EPA to be not as important for prostate cancer, however, because it does not contribute anywhere near as much to the overall radiogenic risk, at least for uniform whole-body radiation (that is averaged over males and females).

Thyroid

EPA's model for thyroid cancer incidence, just like BEIR VII's, is only based on relative risk transport (ERR model); however, the model differs from BEIR VII's and is of the following form:

$$ERR(D, e, t) = \beta\, D\, A(e)\, T(t), \tag{5-14}$$

where A(e) and T(t) are multiplicative factors for age-at-exposure and time-since-exposure, respectively, given in Table 5-3 (taken from Table 3-5 in Blue Book, pg.32). For ages-at-exposure > 15 years, the EPA model borrows from the BEIR VII model, which approximates an 8% per year decrease in ERR with age-at-exposure (*17*).

For calculating LAR of cancer mortality, EPA assumed a simple 5% fatality rate for all radiogenic thyroid cancers (refer to the 2011 EPA Blue Book for specific details on this assumption and the model itself).

Additional Site-Specific Solid Cancers

In addition to the site-specific solid cancers for which BEIR VII calculated LARs of incidence and mortality, the 2011 EPA models include LARs specific to the following sites: kidney, bone, and skin. However, for this specific study, the kidney was applied a different methodology (refer to the section Extensions to the 2011 EPA Models for this Study) than that employed by EPA, so following is a description for the bone and skin sites only.

Skeletal endosteum (bone)

EPA employs an absolute risk model for their estimates of bone cancer, which for small acute doses reduces to the form:

$$\Delta r = \alpha\, D\, g(e)\, h(t), \tag{5-15}$$

where $\alpha = 1.782 \times 10^{-3}$ Gy^{-1}, Δr is the increment in bone cancer incidence from an endosteal dose, D, of α-particle radiation; g(e) reflects the variation in risk with age at exposure (e); and h(t) represents the variation with time after exposure (t). In Equation 5-15

$$g(e) = \exp\,[\,-0.0532\,(e-30)], \tag{5-16}$$

and

$$h(t) = (2\pi\,\sigma^2)^{-1/2} \times \exp\left[-\frac{(\ln(t) - \ln(t_0))^2}{2\sigma^2}\right] \times \frac{1}{t} \tag{5-17}$$

where t_0 is 12.72 years and σ is 0.612. Further details on the development of this model are given in the 2011 EPA Blue Book (*17*).

Skin

EPA adopted a model based on relative risk transport for their risk estimates of skin cancer incidence of the form:

$$ERR_I = 0.2\, D\, (0.88)^{e-7}, \tag{5-18}$$

where D is dose (Gy) and *e* is the age at exposure.

For skin cancer mortality risk projections, the EPA has adopted a simple method which is to force mortality to be 0.03% of the incidence projections

$$ERR_M = (0.03/100)\, ERR_I. \tag{5-19}$$

Even though the method is simple, the decision to employ it required in-depth analysis of data on skin. This work is documented in the 2011 EPA Blue Book (*17*).

It is important to note further issues regarding skin cancers. In the Blue Book (*17*), the total risk of cancer incidence includes only fatal skin cancers and does not include non-fatal cases that could have serious (e.g. disfiguring) consequences. For the latter, there are no reliable statistics from which to form a valid risk prediction model. However, for medical procedures, non-fatal skin cancers are important to the overall risk of cancer incidence. Also, the values given in the 2011 EPA Blue Book are for whole-body irradiation; this presents an issue for estimating risks of radiogenic skin cancer incidence because risks might depend on whether the irradiated portion of the skin is protected from UV (Ultra Violet rays). For nuclear medicine, skin dose could perhaps be considered as "whole-body" and thus that scenario would be acceptable. In contrast, however, for CT and definitely for interventional fluoroscopy, exposures result in only portions of the skin being irradiated.

For these reasons, estimates for risks of radiogenic skin cancer incidence have been excluded from the calculation of the overall risk of cancer incidence. However, the estimates for the risk of radiogenic skin cancer mortality have been included in the calculation of overall risk of cancer mortality since the models for this site are based on fatal skin cancers.

Extensions to the 2011 Environmental Protection Agency Models for Medical Dosimetry Applications

For this thesis, additional sites were also included beyond those given in the 2011 EPA Blue Book. These additional sites were added as they were thought to be of importance under the scope of the medical exam simulations and because of the availability of dose distributions to those sites.

Since additional sites were included, which in the Blue Book were part of the "other solids" or remainder category, then that category had to be changed as well to create a "new remainder" that accounts for the extraction of the sites mentioned above. The total list of

additional sites analyzed on this study, for which LAR was calculated, is the following: bone endosteum, skin, oral cavity, kidney, pancreas, gallbladder, central nervous system (CNS), esophagus, and rectum.

Oral Cavity, Kidney, Pancreas, Gallbladder, Central Nervous System (CNS), Esophagus, Rectum, and New Other Solid (or Remainder)

The development of the models for these sites was performed by Dr. David Pawel from the U.S. EPA (Radiation Protection Division) specifically for this study. They were then coded into Microsoft Office Excel 2007 (*18*) by the author as part of the present study. As mentioned earlier, the kidney site is included in the Blue Book's calculations (*17*) but using a different model not employed in this document and it is thus included in this section. The following is an excerpt taken from a write-up (Appendix B) provided by David Pawel for these sites.

The same type of model used in BEIR VII for ERR was fit using data for these 7 specific cancer sites, i.e., ERR depends on dose (D), cancer site (c), sex(s), age-at-exposure(e), and attained age (a):

$$ERR(D, s, e) = \beta_{c,s}\, D \exp\left[\gamma\,(e-30)/10\right] (a/60)^{\eta}. \quad (5\text{-}20)$$

However, different γ and η parameters were utilized and the β parameter was derived differently (refer to Appendix B for methods and values). Projections of LAR were calculated using methods very similar to those described earlier in the section General Methodology for Calculating Lifetime Attributable Risks (LAR), though the ERR were applied to baseline rates of two populations (U.S. and Japan), rather than just one (U.S.) as in BEIR VII or the Blue Book, and the results combined (refer to Appendix B for an analysis on this procedure).

High-LET (Linear Energy Transfer) Radiation

Since high-LET radiation is not considered under the scope of the medical simulation example (to be analyzed later) of this paper, this short section will just state EPA's modifications

to site-specific risk estimates from low-LET in order to account for the relative biological effectiveness, RBE, of high-LET(mainly α-particles). Simply stated, one would just take the LARs calculated for low-LET radiation and divide by an RBE value to obtain the LARs for high-LET radiation. More detailed information is provided in the 2011 EPA Blue Book (*17*) for high-LET radiation.

EPA's site-specific α-particle risk estimates can be obtained by applying an RBE of 20 to the risk estimates from low-LET radiation for most solid tumors (including breast). The low-dose low-LET radiation risk estimate for bone cancer can be obtained by dividing the risk per Gy for α-particles by an RBE of 10. And finally, an RBE of 2 is used for leukemia (*17*).

Lifetime Attributable Risk Tables

From the EPA revisions described above and the addition of models for site-specific solid cancers, new LAR tables were developed and reported as number of cases per 100,000 persons exposed to a single dose of 0.1 Gy. The tables are displayed in yearly increments for ages-at-exposure 0-20 and every 5 years for ages-at-exposure 25-85. Tables 5-4 (males) and 5-5 (females) display LARs of cancer incidence and Tables 5-6 (males) and 5-7 (females) display LARs of cancer mortality.

Simply stated, to calculate the LARs for different exposure scenarios to low-LET radiation, one would scale the LARs by a ratio of the doses from the different exposure scenarios (i.e. new dose dived by 0.1 since the tables were developed with this dose). This procedure works for all sites except for leukemia, which is based on a linear-quadratic model. For leukemia, one would have to calculate the LAR for very small doses and scale up the answer to the desire magnitude since at very low doses the model approaches more linearity. For example, if one was interested in the LAR of leukemia incidence after exposure to 0.2 Gy to the bone

marrow, one would calculate the LAR using the models for leukemia with a dose of 0.0002 Gy and multiply the answer by 1000.

Table 5-1. BEIR VII preferred ERR and EAR models for estimating site-specific solid cancer incidence and mortality

Cancer Site	No. of Cases	ERR Models [a]				EAR Models [a]			
		β_M [b] (95% CI)	β_F [b] (95% CI)	γ [c]	η [d]	β_M [e] (95% CI)	β_F [e] (95% CI)	γ [c]	η [d]
Stomach	3602	0.21 (0.11, .40)	0.48 (0.31, 0.73)	-0.3	-1.4	4.9 (2.7, 8.9)	4.9 (3.2, 7.3)	-0.41	2.8
Colon	1165	0.63 (0.37, 1.1)	0.43 (0.19, 0.96)	-0.3	-1.4	3.2 (1.8, 5.6)	1.6 (0.8, 3.2)	-0.41	2.8
Liver	1146	0.32 (0.16, 0.64)	0.32 (0.10, 1.0)	-0.3	-1.4	2.2 (1.9, 5.3)	1.0 (0.4, 2.5)	-0.41	4.1 (1.9, 6.4)
Lung	1344	0.32 (0.15, 0.70)	1.40 (0.94, 2.1)	-0.3	-1.4	2.3 (1.1, 5.0)	3.4 (2.3, 4.9)	-0.41	5.2 (3.8, 6.6)
Breast	952	—	0.51 (0.28, 0.83)	0	-2.0	—	9.4 (2.3, 4.9)	-0.51	3.5, 1.1 [f]
Prostate	281	0.12 (<0, 0.69)	—	-0.3	-1.4	0.11 (<0, 1.0)	—	-0.41	2.8
Uterus	875	—	0.055 (<0, 0.22)	-0.3	-1.4	—	1.2 (<0, 2.6)	-0.41	2.8
Ovary	190	—	0.38 (0.10, 1.4)	-0.3	-1.4	—	0.7 (0.2, 2.1)	-0.41	2.8
Bladder	352	0.50 (0.18, 1.4)	1.65 (0.69, 4.0)	-0.3	-1.4	1.2 (0.4, 3.7)	0.75 (0.3, 1.7)	-0.41	6.0 (3.1, 9.0)
Other solid cancers	2969	0.27 (0.15, 0.50)	0.45 (0.27, 0.75)	-0.3	-2.8	6.2 (3.8, 10.0)	4.8 (3.2, 7.3)	-0.41	2.8
Thyroid		0.53 (0.14, 2.0)	1.05 (0.28, 3.9)	-0.83	0				

Notes:

*Estimated parameters with 95% CIs. PY = person-years.

*Table Table 12-2 in BEIR VII report, pg. 272 (*16*)

[a] The ERR or EAR is of the form $\beta s\ D \exp(\gamma e^*)(a/60)^{\eta}$, where D is the dose (Sv), e is age at exposure (years), e* is (e – 30) /10 for $e < 30$ and zero for $e \geq 30$, and a is attained age (years). Models for breast and thyroid cancer are based on e instead of e*, although γ is still expressed per decade.

[b] ERR/Sv for exposure at age 30+ at attained age 60.

[c] Per-decade increase in age at exposure over the range 0–30 years (γ).

[d] Exponent of attained age (η).

[e] EAR per 104 PY-Sv for exposure at age 30+ and attained age 60; these values are for cancer incidence and must be adjusted as described in the text to estimate cancer mortality risks.

[f] The first number is for attained ages less than 50; the second number is for attained ages 50 or greater.

Table 5-2. BEIR VII preferred ERR and EAR models for estimating leukemia incidence and mortality

Parameter	ERR Model [a, b, c]	EAR Model [a, b, c]
β_M	1.1 per Sv (0.1, 2.6)	1.62 deaths per 104 PY-Sv (0.1, 3.6)
β_F	1.2 per Sv (0.1, 2.9)	0.93 deaths per 104 PY-Sv (0.1, 2.0)
γ	-0.40 per decade (-0.78, 0.0)	0.29 per decade (0.0, 0.62)
δ	-0.48 (-1.1, 0.2)	0.0
φ	0.42 (0.0, 0.96)	0.56 (0.31, 0.85)
θ	0.87 per Sv (0.16, 15)	0.88 Sv-1 (0.16, 15)

Notes:
*Estimated parameters with 95% CIs based on likelihood ratio profile.
*Table 12-3 in BEIR VII report, pg. 274 (*16*)

[a] The ERR or EAR is of the form $\beta s\ (D + \theta D^2) \exp [\gamma e^* + \delta \log (t / 25) + \varphi e^* \log (t / 25)]$, where D is the dose to the bone marrow (Sv), e is age at exposure (years), e* is (e – 30) /10 for e < 30 and zero for e $\geq$ 30, and t is time since exposure (years).
[b] Based on analyses of LSS mortality data (1950–2000), with 296 deaths from leukemia.
[c] These models apply only to the period 5 or more years following exposure.

Table 5-3. Estimated ERR/Gy and effect modifiers for age at exposure and time since exposure (TSE) for thyroid cancer risk calculations

	EPA Model [a]
ERR/Gy (β)	10.7
Age-at-exposure: *A(e)*	
<5	1.0
5-9	0.6
10-14	0.2
15-19	0.2 exp[-0.083(e-15)]
20+	0.2 exp[-0.083(e-15)]
TSE: *T(t)*	
<5	0
5-14	1.15
15-19	1.9
20-24	1.2
25-29	1.6
30-40	0.47
40+	0.47

Note: taken from Table 3-5 in Blue Book, pg.*32* (*17*)

[a] For age-at-exposure > 15, the ERR per Gy decreases 8% per year (y^{-1})

Table 5-4. LAR of cancer incidence for males using EPA revised models and additional cancer sites

	Age at exposure (years)																				
Cancer Site	0	1	2	3	4	5	6	7	8	9	10	11	12	13	14	15	16	17	18	19	20
(Males)																					
Stomach	167	162	156	150	144	139	133	128	123	118	114	109	105	101	97	93	90	86	83	80	76
Colon	340	331	321	310	300	291	281	272	263	255	247	239	231	223	216	209	203	196	190	184	178
Liver	102	99	95	92	88	85	82	79	76	73	70	68	65	63	61	58	56	54	52	50	48
Lung	318	308	297	286	276	266	256	247	238	229	221	213	205	198	191	184	177	171	165	159	153
Bladder	218	212	206	199	193	186	180	175	169	164	158	153	148	144	139	135	130	126	122	119	115
Thyroid	122	125	127	129	131	107	81	83	84	86	58	29	30	30	31	31	29	28	26	24	22
Bone	10	10	9	9	8	8	8	7	7	6	6	6	5	5	5	5	4	4	4	4	4
Skin	1739	1544	1359	1197	1053	927	816	718	632	556	490	431	379	334	294	259	228	201	177	156	137
Oral Cavity	27	27	26	25	25	24	23	22	22	21	20	20	19	19	18	18	17	17	16	16	15
Kidney	21	21	20	19	19	18	18	17	17	16	16	15	15	14	14	14	13	13	12	12	12
Pancreas	17	16	16	16	15	15	14	14	13	13	13	12	12	12	11	11	11	10	10	10	9
Gallbladder	1.4	1.4	1.3	1.3	1.2	1.2	1.2	1.1	1.1	1.1	1.0	1.0	1.0	0.9	0.9	0.9	0.9	0.8	0.8	0.8	0.8
CNS/Brain	16	15	15	14	14	14	13	13	12	12	12	11	11	11	10	10	10	10	9	9	9
Esophagus	13	13	12	12	12	11	11	11	10	10	10	10	9	9	9	8	8	8	8	8	7
Rectum	15	15	15	14	14	13	13	13	12	12	12	11	11	11	10	10	10	9	9	9	9
Prostate	196	192	186	181	176	170	133	161	156	151	147	142	138	134	130	126	123	119	116	112	109
Leukemia	193	182	170	160	150	142	134	128	122	117	112	108	105	102	99	97	95	93	92	90	89
Remainder	444	435	422	410	398	386	375	364	353	343	333	323	313	304	295	287	278	270	263	255	248

Note: Number of cases per 100,000 persons exposed to a single dose of 0.1 Gy. These estimates have been adjusted by a DDREF of 1.5, except for bone, skin, and leukemia.

Table 5-4. Continued

	Age at exposure (years)												
Cancer Site	25	30	35	40	45	50	55	60	65	70	75	80	85
(Males)													
Stomach	63	51	50	48	46	43	39	35	30	24	18	12	7
Colon	151	128	127	125	122	117	108	97	82	66	48	30	16
Liver	40	33	33	32	31	29	27	24	21	17	13	9	6
Lung	128	107	107	107	106	103	98	90	79	65	50	35	22
Bladder	98	84	84	83	83	81	77	70	61	50	37	24	13
Thyroid	16	11	8	5	3	2	1	1	0	0	0	0	0
Bone	3	2	2	1	1	1	0	0	0	0	0	0	0
Skin	73	39	20	11	6	3	2	1	0	0	0	0	0
Oral Cavity	13	11	10	9	7	6	4	3	2	1	1	0	0
Kidney	10	8	8	7	6	5	4	3	2	1	1	0	0
Pancreas	8	7	7	6	6	5	4	3	2	2	1	0	0
Gallbladder	0.7	0.6	0.6	0.5	0.5	0.5	0.4	0.3	0.2	0.1	0.1	0.0	0.0
CNS/Brain	8	5	4	3	3	2	2	1	1	1	0	0	0
Esophagus	6	5	5	5	5	4	3	3	2	1	1	0	0
Rectum	7	6	6	5	5	4	4	3	2	1	1	0	0
Prostate	95	82	82	83	83	80	73	61	45	30	17	9	4
Leukemia	84	78	78	79	80	83	85	88	89	88	80	64	45
Remainder	215	178	171	162	152	140	124	105	85	64	44	26	14

Note: Number of cases per 100,000 persons exposed to a single dose of 0.1 Gy. These estimates have been adjusted by a DDREF of 1.5, except for bone, skin, and leukemia.

Table 5-5. LAR of cancer incidence for females using EPA revised models and additional cancer sites

	Age at exposure (years)																				
Cancer Site	0	1	2	3	4	5	6	7	8	9	10	11	12	13	14	15	16	17	18	19	20
(Females)																					
Stomach	211	204	196	189	182	175	168	161	155	149	143	138	133	127	122	118	113	109	105	100	96
Colon	224	219	212	205	198	192	186	180	174	168	163	158	153	148	143	138	134	130	125	121	117
Liver	57	55	53	51	49	47	45	43	42	40	39	37	36	34	33	32	31	29	28	27	26
Lung	780	758	731	705	680	656	633	611	590	569	549	530	511	493	476	459	443	428	413	399	385
Bladder	220	214	207	201	194	188	182	176	171	165	160	155	150	145	140	136	132	127	123	120	116
Thyroid	382	395	405	415	426	349	269	275	281	288	196	100	102	103	105	106	99	92	85	79	73
Bone	10	10	9	9	8	8	8	7	7	6	6	6	6	5	5	5	4	4	4	4	4
Skin	1003	888	782	688	606	533	469	413	364	320	282	248	218	192	169	149	131	115	101	89	79
Oral Cavity	18	18	17	17	16	16	15	15	15	14	14	13	13	13	12	12	11	11	11	11	10
Kidney	16	16	15	15	14	14	14	13	13	12	12	12	11	11	11	10	10	10	10	9	9
Pancreas	19	18	18	17	17	16	16	15	15	15	14	14	13	13	13	12	12	11	11	11	11
Gallbladder	1.9	1.8	1.8	1.7	1.7	1.6	1.6	1.5	1.5	1.5	1.4	1.4	1.3	1.3	1.3	1.2	1.2	1.1	1.1	1.1	1.0
CNS/Brain	18	17	17	16	16	15	15	14	14	14	13	13	12	12	12	11	11	11	10	10	10
Esophagus	4.1	4.0	3.8	3.7	3.6	3.5	3.4	3.3	3.2	3.1	3.0	2.9	2.9	2.8	2.7	2.6	2.5	2.5	2.4	2.3	2.2
Rectum	15	14	14	14	13	13	12	12	12	11	11	11	10	10	10	9	9	9	9	8	8
Breast	1254	1199	1140	1083	1030	979	930	884	840	798	759	721	685	650	618	587	558	530	503	478	453
Ovary	91	88	85	82	79	77	74	71	69	66	64	62	60	57	55	53	51	50	48	46	44
Uterus	65	63	61	59	57	55	53	51	49	47	45	44	42	41	39	38	36	35	34	32	31
Leukemia	172.5	159	147	136	126	117	110	103	97	92	88	85	82	79	77	75	73	72	71	69	68
Remainder	761	743	722	701	680	660	641	622	604	586	569	552	536	520	505	490	476	462	448	435	423

Note: Number of cases per 100,000 persons exposed to a single dose of 0.1 Gy. These estimates have been adjusted by a DDREF of 1.5, except for bone, skin, and leukemia.

Table 5-5. Continued

	Age at exposure (years)												
Cancer Site	25	30	35	40	45	50	55	60	65	70	75	80	85
(Females)													
Stomach	79	64	63	61	58	55	51	46	40	33	25	18	11
Colon	100	84	83	82	79	76	71	65	56	46	35	23	12
Liver	22	18	18	17	17	16	15	14	12	10	8	6	4
Lung	323	270	269	267	263	254	239	216	185	150	112	77	48
Bladder	98	84	83	82	81	78	73	67	58	47	36	24	14
Thyroid	48	31	19	12	7	4	2	1	1	0	0	0	0
Bone	3	2	2	1	1	1	0	0	0	0	0	0	0
Skin	42	22	12	6	3	2	1	0	0	0	0	0	0
Oral Cavity	9	7	6	5	4	3	3	2	1	1	1	0	0
Kidney	8	6	6	5	4	4	3	2	2	1	1	0	0
Pancreas	9	8	7	7	6	6	5	4	3	3	2	1	0
Gallbladder	0.9	0.8	0.7	0.7	0.6	0.6	0.5	0.5	0.4	0.3	0.2	0.1	0.1
CNS/Brain	8	6	5	4	3	3	2	1	1	1	0	0	0
Esophagus	1.9	1.6	1.6	1.5	1.4	1.3	1.1	0.9	0.7	0.5	0.3	0.2	0.1
Rectum	7	6	5	5	4	4	3	2	2	1	1	0	0
Breast	348	265	199	147	105	73	50	33	21	13	7	4	2
Ovary	37	31	30	28	26	24	21	17	14	11	7	4	2
Uterus	25	21	20	19	18	16	14	12	10	8	6	4	2
Leukemia	64	60	60	61	62	63	64	65	65	63	57	47	34
Remainder	365	302	289	274	256	235	210	181	150	117	84	52	28

Note: Number of cases per 100,000 persons exposed to a single dose of 0.1 Gy. These estimates have been adjusted by a DDREF of 1.5, except for bone, skin, and leukemia.

Table 5-6. LAR of cancer mortality for males using EPA revised models and additional cancer sites

	Age at exposure (years)																				
Cancer Site	0	1	2	3	4	5	6	7	8	9	10	11	12	13	14	15	16	17	18	19	20
(Males)																					
Stomach	85	82	79	76	73	70	67	65	62	60	58	55	53	51	49	47	46	44	42	40	39
Colon	153	149	144	140	135	131	126	122	118	115	111	107	104	101	97	94	91	88	85	83	80
Liver	78	76	73	70	68	65	63	60	58	56	54	52	50	48	46	45	43	41	40	38	37
Lung	291	283	272	262	253	244	235	226	218	210	202	195	188	181	174	168	162	156	151	146	140
Bladder	43	42	41	39	38	37	36	34	33	32	31	30	29	28	27	26	26	25	24	23	23
Thyroid	6.1	6.2	6.3	6.4	6.6	5.3	4.1	4.1	4.2	4.3	2.9	1.5	1.5	1.5	1.5	1.6	1.5	1.4	1.3	1.2	1.1
Bone	3.6	3.5	3.3	3.1	2.9	2.8	2.6	2.5	2.4	2.2	2.1	2.0	1.9	1.8	1.7	1.6	1.5	1.4	1.4	1.3	1.2
Skin	0.5	0.5	0.4	0.4	0.3	0.3	0.2	0.2	0.2	0.2	0.1	0.1	0.1	0.1	0.1	0.1	0.1	0.1	0.1	0.0	0.0
Oral Cavity	5.9	5.8	5.6	5.5	5.3	5.1	5.0	4.8	4.7	4.6	4.4	4.3	4.2	4.1	3.9	3.8	3.7	3.6	3.5	3.4	3.3
Kidney	6.2	6.1	5.9	5.7	5.5	5.4	5.2	5.1	4.9	4.8	4.6	4.5	4.4	4.2	4.1	4.0	3.9	3.8	3.7	3.6	3.5
Pancreas	15	15	14	14	13	13	13	12	12	12	11	11	11	10	10	10	9	9	9	9	8
Gallbladder	0.8	0.8	0.8	0.8	0.7	0.7	0.7	0.7	0.6	0.6	0.6	0.6	0.6	0.6	0.5	0.5	0.5	0.5	0.5	0.5	0.5
CNS/Brain	10	10	10	10	9	9	9	9	8	8	8	8	7	7	7	7	7	6	6	6	6
Esophagus	13	12	12	12	11	11	11	10	10	10	9	9	9	9	8	8	8	8	7	7	7
Rectum	2.8	2.7	2.7	2.6	2.5	2.4	2.4	2.3	2.2	2.2	2.1	2.0	2.0	1.9	1.9	1.8	1.8	1.7	1.7	1.6	1.6
Prostate	28	27	26	25	25	24	65	22	22	21	21	20	19	19	18	18	17	17	16	16	15
Leukemia	65	65	65	65	65	65	65	65	65	65	64	64	64	63	63	62	62	62	61	61	60
Remainder	203	199	193	187	182	176	171	166	161	157	152	147	143	139	135	131	127	123	120	117	113

Note: Number of cases per 100,000 persons exposed to a single dose of 0.1 Gy. These estimates have been adjusted by a DDREF of 1.5, except for bone, skin, and leukemia.

Table 5-6. Continued

	Age at exposure (years)												
Cancer Site	25	30	35	40	45	50	55	60	65	70	75	80	85
(Males)													
Stomach	32	26	25	25	24	22	21	19	17	14	11	8	5
Colon	68	58	58	57	56	54	51	47	41	35	27	19	12
Liver	31	25	25	25	24	23	22	21	19	16	13	9	6
Lung	117	98	98	98	97	95	91	84	75	63	50	35	22
Bladder	19	16	17	17	17	17	16	16	15	14	12	10	7
Thyroid	0.8	0.6	0.4	0.3	0.2	0.1	0.1	0.0	0.0	0.0	0.0	0.0	0.0
Bone	0.9	0.7	0.5	0.4	0.3	0.2	0.1	0.1	0.1	0.0	0.0	0.0	0.0
Skin	0.0	0.0	0.0	0.0	0.0	0.0	0.0	0.0	0.0	0.0	0.0	0.0	0.0
Oral Cavity	2.9	2.4	2.3	2.1	1.8	1.5	1.2	0.9	0.6	0.4	0.3	0.1	0.1
Kidney	3.0	2.5	2.4	2.3	2.1	1.8	1.5	1.2	0.9	0.6	0.4	0.2	0.1
Pancreas	7	6	6	6	5	5	4	3	2	2	1	1	0
Gallbladder	0.4	0.3	0.3	0.3	0.3	0.3	0.2	0.2	0.1	0.1	0.0	0.0	0.0
CNS/Brain	5	4	3	3	2	2	1	1	1	0	0	0	0
Esophagus	6	5	5	5	5	4	3	2	2	1	1	0	0
Rectum	1.4	1.1	1.1	1.0	0.9	0.8	0.7	0.6	0.5	0.3	0.2	0.1	0.1
Prostate	13	11	12	12	12	12	12	12	12	11	10	8	5
Leukemia	59	57	59	61	64	67	71	76	80	81	76	64	46
Remainder	98	84	83	82	80	76	70	62	53	43	32	21	12

NOTE: Number of cases per 100,000 persons exposed to a single dose of 0.1 Gy. These estimates have been adjusted by a DDREF of 1.5, except for bone, skin, and leukemia.

Table 5-7. LAR of cancer mortality for females using EPA revised models and additional cancer sites

	Age at exposure (years)																				
Cancer Site	0	1	2	3	4	5	6	7	8	9	10	11	12	13	14	15	16	17	18	19	20
(Females)																					
Stomach	112	108	104	100	96	93	89	86	82	79	76	73	70	68	65	63	60	58	56	53	51
Colon	96	93	90	87	84	82	79	77	74	72	69	67	65	63	61	59	57	55	54	52	50
Liver	48	47	45	43	41	40	38	37	36	34	33	32	30	29	28	27	26	25	24	23	22
Lung	638	619	597	576	556	536	517	499	481	464	448	432	417	402	388	374	361	349	337	325	314
Bladder	57	56	54	52	51	49	47	46	44	43	42	40	39	38	37	35	34	33	32	31	30
Thyroid	19	20	20	21	21	17	13	14	14	14	10	5	5	5	5	5	5	5	4	4	4
Bone	3.6	3.5	3.3	3.1	3.0	2.8	2.7	2.5	2.4	2.3	2.1	2.0	1.9	1.8	1.7	1.6	1.6	1.5	1.4	1.3	1.2
Skin	0.3	0.3	0.2	0.2	0.2	0.2	0.1	0.1	0.1	0.1	0.1	0.1	0.1	0.1	0.1	0.0	0.0	0.0	0.0	0.0	0.0
Oral Cavity	3.4	3.3	3.2	3.1	3.1	3.0	2.9	2.8	2.7	2.6	2.6	2.5	2.4	2.3	2.3	2.2	2.1	2.1	2.0	2.0	1.9
Kidney	4.2	4.1	4.0	3.9	3.7	3.6	3.5	3.4	3.3	3.2	3.1	3.0	2.9	2.9	2.8	2.7	2.6	2.5	2.5	2.4	2.3
Pancreas	16	16	16	15	15	14	14	13	13	13	12	12	12	11	11	11	10	10	10	9	9
Gallbladder	1.0	1.0	1.0	1.0	0.9	0.9	0.9	0.8	0.8	0.8	0.8	0.8	0.7	0.7	0.7	0.7	0.6	0.6	0.6	0.6	0.6
CNS/Brain	11	11	10	10	10	9	9	9	9	8	8	8	8	7	7	7	7	7	6	6	6
Esophagus	3.4	3.3	3.2	3.1	3.0	2.9	2.9	2.8	2.7	2.6	2.5	2.5	2.4	2.3	2.3	2.2	2.1	2.1	2.0	1.9	1.9
Rectum	2.5	2.4	2.4	2.3	2.2	2.2	2.1	2.0	2.0	1.9	1.9	1.8	1.8	1.7	1.7	1.6	1.6	1.5	1.5	1.4	1.4
Breast	427	409	389	369	351	334	317	301	286	272	259	246	234	222	211	201	190	181	171	162	153
Ovary	56	54	52	51	49	47	46	44	43	41	40	39	38	36	35	34	33	32	31	30	29
Uterus	17	16	16	15	14	14	13	13	12	12	11	11	11	10	10	10	9	9	9	8	8
Leukemia	53	53	52	52	51	51	51	51	50	50	50	50	49	49	49	49	48	48	48	48	48
Remainder	400	391	380	369	358	347	337	327	318	308	299	290	282	274	265	258	250	243	236	229	222

NOTE: Number of cases per 100,000 persons exposed to a single dose of 0.1 Gy. These estimates have been adjusted by a DDREF of 1.5, except for bone, skin, and leukemia.

Table 5-7. Continued

	Age at exposure (years)												
Cancer Site	25	30	35	40	45	50	55	60	65	70	75	80	85
(Females)													
Stomach	42	34	33	33	31	30	28	26	23	20	17	13	9
Colon	43	36	36	35	34	33	32	29	27	23	19	14	9
Liver	18	15	15	15	15	14	14	13	12	10	8	6	4
Lung	263	220	220	219	215	209	199	182	160	134	106	76	49
Bladder	26	22	22	22	22	21	21	20	19	18	16	12	9
Thyroid	2	2	1	1	0	0	0	0	0	0	0	0	0
Bone	1.0	0.7	0.5	0.4	0.3	0.2	0.2	0.1	0.1	0.0	0.0	0.0	0.0
Skin	0.0	0.0	0.0	0.0	0.0	0.0	0.0	0.0	0.0	0.0	0.0	0.0	0.0
Oral Cavity	1.6	1.3	1.2	1.1	1.0	0.9	0.7	0.6	0.4	0.3	0.2	0.2	0.1
Kidney	2.0	1.7	1.6	1.5	1.4	1.2	1.1	0.9	0.7	0.5	0.3	0.2	0.1
Pancreas	8	7	6	6	6	5	5	4	3	3	2	1	1
Gallbladder	0.5	0.4	0.4	0.4	0.4	0.3	0.3	0.3	0.2	0.2	0.1	0.1	0.0
CNS/Brain	5	4	4	3	3	2	2	1	1	1	0	0	0
Esophagus	1.6	1.4	1.4	1.3	1.2	1.1	1.0	0.8	0.6	0.5	0.3	0.2	0.1
Rectum	1.2	1.0	0.9	0.9	0.8	0.7	0.6	0.5	0.4	0.3	0.3	0.2	0.1
Breast	115	85	60	42	28	17	10	6	3	2	1	0	0
Ovary	24	21	20	20	19	18	17	15	13	10	7	5	3
Uterus	6	5	5	5	5	5	5	4	4	3	3	2	2
Leukemia	47	46	47	48	50	53	55	57	59	59	56	48	37
Remainder	192	163	160	156	150	142	132	119	103	84	63	41	24

NOTE: Number of cases per 100,000 persons exposed to a single dose of 0.1 Gy. These estimates have been adjusted by a DDREF of 1.5, except for bone, skin, and leukemia.

CHAPTER 6
MEDICAL IMAGING SIMULATION-FDG PET/CT SCANS

The medical example simulated in this study was a typical ^{18}F-FDG PET/CT exam. In this procedure, the patient receives internal exposure from the PET (Positron Emission Tomography) component via the ^{18}F radionuclide (with doses from the emitted positrons and the resulting two annihilation photons), and external exposure from the x-rays emitted by the CT (Computed Tomography). The medical scenario was simulated through the use of Monte Carlo radiation transport simulation using the MCNPX code and the UF (University of Florida) series of computational hybrid phantoms. Further details are given in Appendix C for each simulation.

The internal dosimetry from the ^{18}F-FDG PET component of the simulation was coded, and provided, by Mike Wayson (Ph.D. candidate-Medical Physics, ALRADS) from the University of Florida. The external dosimetry for the CT component of the simulation was coded, and provided, by Daniel Long (MS Student-Medical Physics, ALRADS) from the University of Florida. Appendix C provides further details as provided by these authors.

The risks from the overall procedure were calculated by utilizing the dosimetry obtained from each component of the simulation, and then adding the risks from the PET component and the CT component.

Results

LAR models require that the organ doses be provided in units of Sv (unit of organ equivalent doses). The doses obtained from the PET component of the simulation were in Sv, so they were readily applied to the LAR models. The doses obtained from the CT component, however, were given in Gy (unit of organ absorbed doses). As mentioned in Chapter 2, the radiation weighting factor for photons and their secondary electrons is unity, and then the

absorbed dose to organ in Gy is numerically equivalent to the corresponding organ equivalent dose in Sv. Doses obtained from the simulation can be found in Appendix D (in units of mSv).

For the purpose of comparison, risks of cancer incidence and mortality are displayed separately in this study. However, it was deemed more appropriate to analyze only mortality risks in order to obtain a better contrast with the effective dose-derived radiation detriment (Chapter 3), as a lethality fraction is an integral part of the ICRP Publication103 detriment concept, among other stochastic endpoints such as cancer mortality, cancer morbidity, and years of life lost. In the case illustrated in this work, the LARs for each organ site, calculated from EPA revised models with the organ doses obtained from the Monte Carlo simulations, were summed across all organs to give the overall LAR of cancer (incidence or mortality) for males and females (separately) with ages-at-exposure of 0 (new born), 1, 5, 10, 15, and 30 years old. To estimate LARs for ages-at-exposure $\geq$ 30 years, it was assumed that the change in dosimetry for older ages was minimal and thus the dose distributions obtained for age 30 were further used for simulated patients of ages 30 to 80 years. The reader is reminded that, as mentioned in Chapter 5, radiogenic risks of skin cancer incidence were not included in the overall risk of cancer incidence. However risks of skin cancer mortality were included in the overall risk of cancer mortality (refer to Chapter 5 for details).

The previous approach was then compared with an overall "risk" estimate derived from the effective dose using ICRP Publication 103 tissue weighting factors. In order to be able implement the latter method and compare it with LARs, the effective doses obtained (Appendix D) were corrected using a detriment adjusted nominal risk coefficient for cancer incidence for the whole population that is reported in ICRP Publication 103 as 5.5×10^{-2} Sv^{-1} (*11*). This value was multiplied by the effective dose to give an effective dose-derived overall "risk" of cancer. It

must be noted that the answer yielded by the effective dose method is not necessarily a risk, but rather ICRP 103's quantity referred to as radiation detriment. The goal of this paper is not to compare these two quantities (LAR and radiation detriment) as if they both represent the same risk values, but rather the opposite; it is the belief of the author that the LAR approach is much more transparent and subject to better interpretation.

Furthermore, since effective dose calculations use sex-and-age averaged tissue weighting factors, the effect of using sex-averaged versus sex-specific LAR values was also examined. To accomplish this, the following equation from the *Blue Book* (*17*) was utilized:

$$LAR_{AVG}(D,e) = \frac{1.048 S_{MALE}(e) LAR_{MALE}(D,e) + S_{FEMALE}(e) LAR_{FEMALE}(D,e)}{1.048 S_{MALE} + S_{FEMALE}} \quad (6\text{-}1)$$

where LAR_{AVG} is the sex-averaged LAR, LAR_{MALE} and LAR_{FEMALE} are the LARs obtained for males and female respectively. The parameter 1.048 is the ratio of the male to female births. S (e) is the probability of surviving until age-at-exposure e (from birth).

The results of all the calculations previously described are given in Appendix E. Table E-1 presents the overall (summed across all organs) risk of cancer (incidence and mortality) for the PET component of the medical simulation; Table E-3 presents the overall risks of cancer from the CT component. Tables E-2 (PET) and E-4 (CT) present the risks as ratios of all the risks to the risk for the 30-year old adult male (incidence and mortality) for a better observation on the effects of sex and age averaging on the values. Table E-5 displays the results of the entire procedure (PET results plus the CT results) and Table E-6 presents those results as ratios as previously described.

Discussion

As mentioned in the Results section, even though risks of cancer incidence and mortality were displayed, it was deemed more appropriate to only analyze mortality risks in order to obtain

a better contrast with the effective dose-derived radiation detriment. To better visualize the differences between both methodologies (LAR of cancer mortality and radiation detriment calculations), Figures 6-1(results for PET), 6-2 (results for CT), and 6-3 (combined results) were produced from Tables E-1, E-3, and E-5 respectively (from Appendix E). They display the overall LAR of cancer mortality (as number of excess cases per 100,000 individuals exposed) for males, females, a sex-average of these two values (Equation 6-1), and the radiation detriment value obtained by using effective dose calculations. Figures for LARs of cancer incidence are provided in Appendix E.

For purposes of risk analysis, ages-at-exposure 0 through 15 years old will be considered pediatrics, while ages 30 through 80 will be considered adults. Although the dose distributions (Appendix D) from the PET and CT simulations, separately, were very similar for males and females, there are clear differences present when observing the age-and-sex specific lifetime attributable risk estimates presented in the figures. Mainly, larger risks for females than for males are observed, indicating a larger overall risk of cancer for females than for males from the entire PET/CT procedure – a trend also observed in the LARs for most cancer sites in BEIR VII (*16*).

LARs of cancer mortality were an average of 1.78 times higher for pediatric females, compared to males, on the PET component of the simulation, and an average of 1.38 times for adults. For the CT component of the simulation, LARs of cancer mortality were an average of 1.87 times higher for pediatric females, compared to males, and an average of 1.45 times for adults. Even though the differences in LAR between sexes are somewhat reduced, as illustrated by the averages, for older ages-at-exposure, what this demonstrates is the fact that averaging across sexes is an erroneous approach to risk quantification, resulting, in this specific simulation,

in an overestimation of cancer risk for males, and underestimation of risk for females. The following discussion is for ages-at-exposure up to age 30.

For the PET component of the simulation, referring to Figure 6-1, differences in age-specific risks and radiation detriment are more emphasized in newborns than the rest of ages-at-exposure. For the newborn, the estimate for radiation detriment is much lower than the LAR for males (2.02 times lower) and females (3.68 times lower) and continues to be lower for older ages-at-exposure, but the difference starts to decrease with increasing age up until age-at-exposure 30. This implies that for the PET part of the imaging procedure, radiation detriment underestimates the overall LAR of cancer mortality in pediatrics and starts to approach LARs for adults up to age 30. Administered activity of the FDG is adjusted by body weight and thus the resulting organ equivalent doses, along with the associated risks, vary with age, gender, and body composition. This is illustrated by Figure 6-1 in the different LARs of cancer mortality across ages. In this figure, the overall LARs for pediatrics are higher than the risks for adults; this is because children are generally more radiosensitive and have their entire lifetimes to develop radiation-induced effects (*5*).

For the CT component of the simulation, referring to Figure 6-2, risks of cancer mortality increase steadily up until age-at-exposure 5 and then begin to decrease for ages-at-exposure ≥10 years. Techniques for CT imaging are adjusted to account for the individual's physical composition (e.g. height and weight); generally, as people get older they tend to get taller and bigger (at least between the ages 0-15) therefore receiving a higher dose from CT imaging. As observed in Figure 6-2, this technique adjustment has a bigger impact in pediatric than in adult patients since the physical changes undergone by pediatrics are more drastic during the time-span of 0-15 years than the changes adults could experience from 30-80 years of age; however,

the difference in doses (Appendix D) resulting from these physical changes are not so high as to "overpower" the general tendency for LAR to decrease with increasing ages-at-exposure and hence the LAR resumes this trend for ages-at-exposure ≥10 years as illustrated by Figure 6-2. Just as it was observed with the PET component of the simulation, radiation detriment underestimates the overall LAR of cancer mortality in pediatrics and starts to approach LAR values up to age 30 for the CT component; as an example, it can be observed with the newborns that the estimate for radiation detriment is much lower than the LAR for males (1.73 times lower) and females (3.35 times lower).

For ages-at-exposure above 30 years, a very interesting trend is observed that merits special mention. As explained earlier in the Results section, the dose distributions obtained for age 30 were used for exposure ages 30 through 80 years old. This approach further emphasizes the ineffectiveness of the effective dose-derived radiation detriment method for risk analysis as illustrated in Figures 6-1, 6-2, and 6-3. Since the same dose distributions were used for the adults, the radiation detriment method assumes the same "risks" of cancer mortality across that age group and consistently overestimates the "risk" of cancer, when compared to LAR methodology. This in part due to the fact that this quantity does not have a way to account for different factors that influence risk, such as latency periods, (refer to Chapter 5) – solid cancers have an average latency period of 5 years and leukemia of 2 – or the fact that the older a patient is when exposed, the lower the risk of cancer induction is, and mortality from that cancer, since the patient will have less time to develop or show a cancer over the rest of their lifetimes. The LARs obtained from the EPA revised models portray this perfectly as they continue to decrease with age-at-exposure.

When analyzing the results from both procedures combined (PET/CT), in Figure 6-3, it can be observed that the overall risks for the procedure are dominated by the PET component for pediatric ages-at-exposure and follow the general tendency for LAR to decrease with increasing ages-at-exposure as it was noted with both components, PET and CT, separately. From this, it can be resolved that, for the entire procedure, radiation detriment underestimates risks of cancer mortality for pediatrics and generally overestimates the risks for adults.

From the previous discussion, it is evident that radiation detriment is very inconsistent across ages and sexes and is thus an unfit quantity to assess individual risks of cancer for medical imaging procedures such as nuclear medicine (PET), fluoroscopy, and computed tomography (CT).

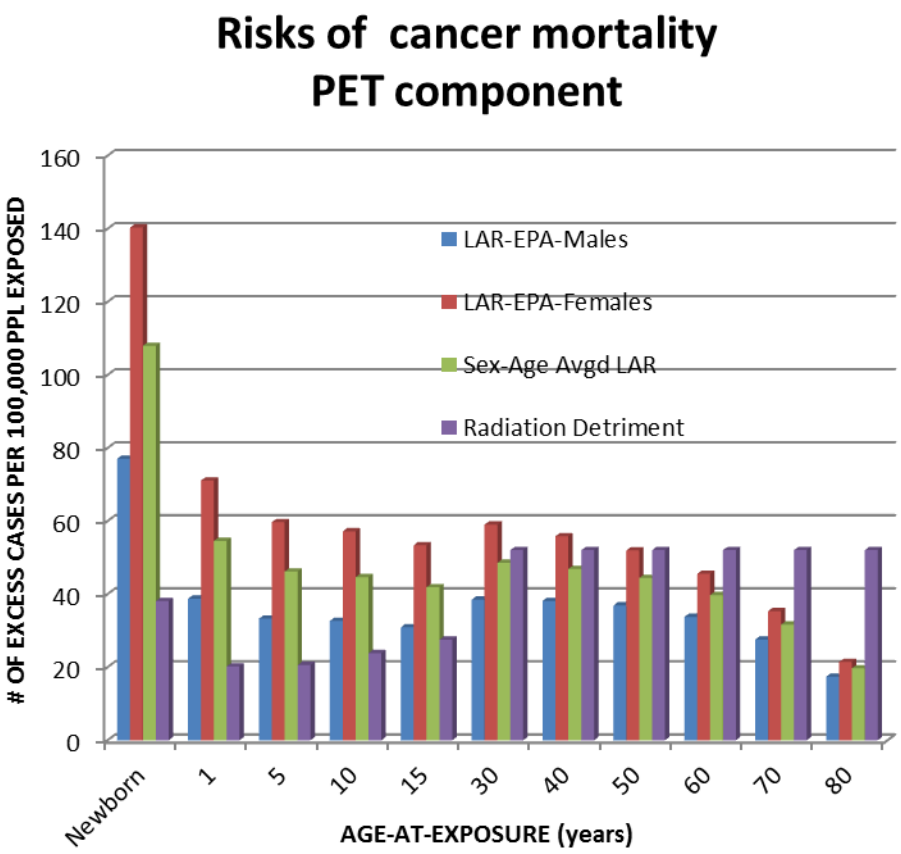

Figure 6-1. Lifetime attributable risks of cancer mortality and radiation detriment from the PET component of the simulation

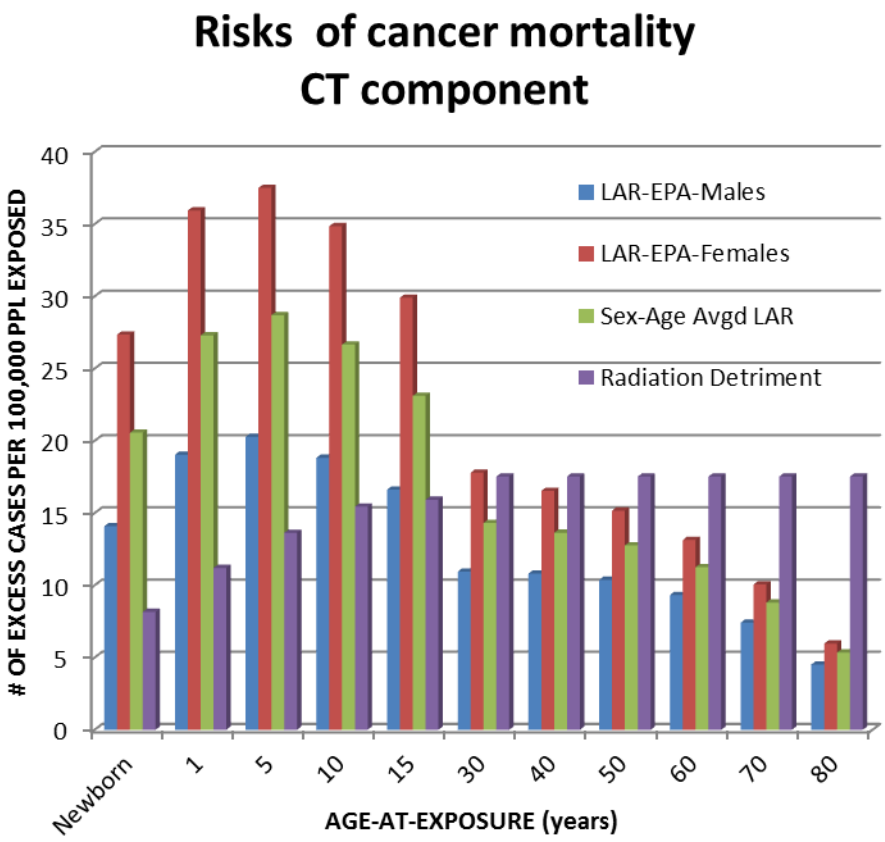

Figure 6-2. Lifetime attributable risks of cancer mortality and radiation detriment from the CT component of the simulation

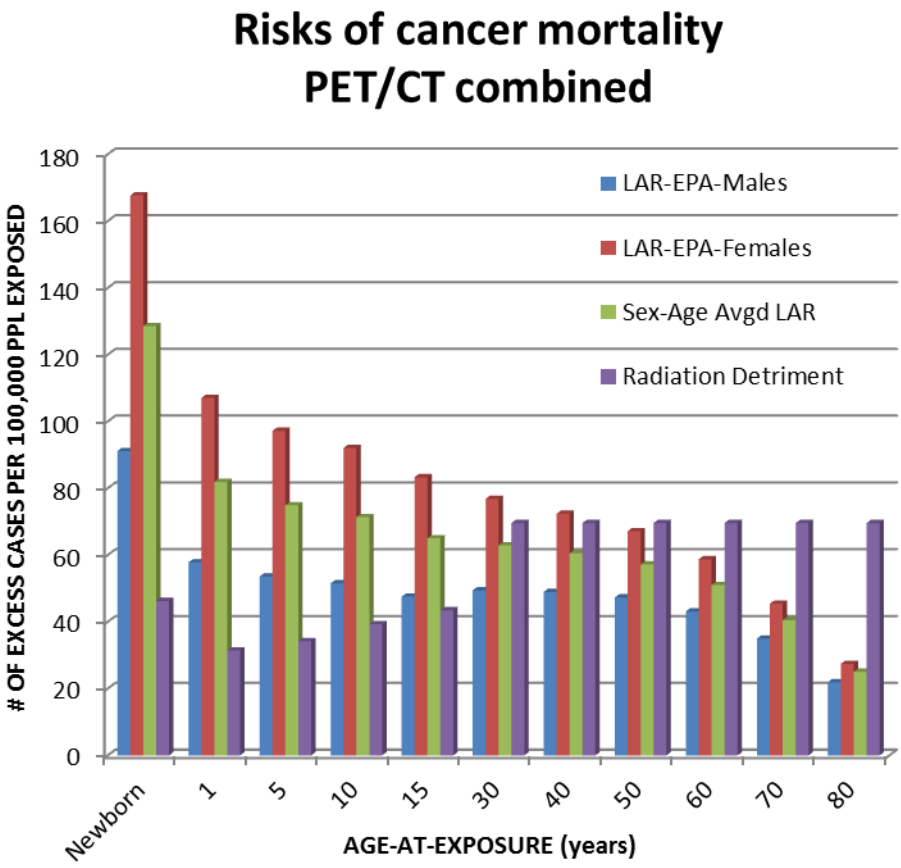

Figure 6-3. Combined (PET/CT) lifetime attributable risks of cancer mortality and radiation detriment

CHAPTER 7
CONCLUSIONS

Through the use of the Environmental Protection Agency (EPA) LAR models, which uses BEIR VII models for calculating lifetime attributable risks, but with some modifications and extensions, risks of radiation-induced cancer (incidence and mortality) were calculated for an ^{18}F-FDG PET/CT imaging procedure. The revised EPA risk models were implemented for the purpose of providing age and gender dependent LAR tables needed to better quantify stochastic risk in medical imaging studies. This approach to risk quantification was then contrasted to the use of the ICRP (International Commission on Radiological Protection) effective dose-derived radiation detriment, a quantity with limited application to medical radiation exposure.

Dose distributions were obtained separately for the PET component of the simulation, and for the CT component. Results were obtained from these components and then combined to provide an overall LAR of cancer (incidence and mortality) for ages-at-exposure 0, 1, 5, 10, 15, and 30. To estimate LARs for ages-at-exposure $\geq$ 30 years, it was assumed that the change in dosimetry for older ages was minimal and thus the dose distributions obtained for age 30 were used for ages 30 through 80 years old. This document only analyzed risks of cancer mortality; this was deemed a more appropriate approach for comparison against radiation detriments since a lethality fraction is part of the ICRP 103 detriment concept, among other stochastic endpoints such as cancer mortality, cancer morbidity, and years of life lost.

In order to be able implement the radiation detriment method and compare it with EPA-derived LARs, the effective doses obtained were corrected using a detriment adjusted nominal risk coefficient for the whole population that is reported in ICRP 103 as 5.5×10^{-2} Sv^{-1} (*11*).

For both parts of the imaging procedure (PET and CT separately), radiation detriment underestimates the overall LAR of cancer mortality in pediatrics (< 30 years old) and starts to

approach LARs for adults at age 30. For exposure ages 30 through 80 years old, radiation detriment consistently overestimates the risk of cancer and erroneously provides the same risk index for all the ages in the adult group. From the overall LARs it was observed, for this particular example (PET/CT combined), that averaging across sexes and ages results in both overestimation, for males, and underestimation, for females, of risks of cancer-induced mortality to individuals; radiation detriment resulted in an overall risk underestimation for pediatrics and overestimation for adults. Therefore, it is concluded here that sex- and age-averaging, along with the radiation detriment technique of "risk" quantification, are very inconsistent methods and are thus unfit quantities to assess individual risks of radiogenic cancer for medical imaging procedures such as nuclear medicine, fluoroscopy, and computed tomography.

It is important to note that these trends were observed only for this particular example and more data (simulations and risk calculations) would be needed in order to generalize them to other medical imaging procedures. It is the belief of the author that the EPA's LAR approach to sex-and-age specific stochastic risk quantification is much more transparent and subject to better interpretation than using ICRP 103's effective dose method, which yields radiation detriments and not necessarily risks of radiation-induced cancer.

It is important to note once more that the ICRP clearly states in its Publication 103 that effective dose is intended for use as a protection quantity, mainly used for prospective dose assessment for planning and optimization in radiological protection, and demonstration of compliance with dose limits for regulatory purposes (*11*). ICRP affirms that "Effective dose is not recommended for epidemiological evaluations, nor should it be used for detailed specific retrospective investigations of individual exposure and risk" (*11*). Furthermore, ICRP states that "risk assessment for medical diagnosis and treatment using ionising radiation is best evaluated

using appropriate risk values for the individual tissues at risk and for the age and sex distribution of the individuals undergoing the medical procedures." (*11*, *12*) However, due to the lack of a better quantity, effective dose has been used in the medical community as a method for estimating stochastic risks from medical imaging procedures since it is the only quantity that offers a relationship between dose and "risk".

This paper is not meant to be interpreted as new standards for stochastic risk quantification from medical imaging procedures. Although the risk estimates obtained using EPA's LAR models have high uncertainties for individual patients, they can be used collectively in optimizing values of exposure (from CT) or administered activity (from PET), and resulting organ doses, to perhaps minimize the risk of radiation-induced cancer while still obtaining good quality images. Furthermore, it is important to note that the w_T from ICRP are for a population of individuals and not for specific individual patients. Similarly, the LAR values are also population based, but are taken for a subset of populations of persons of one sex and of a given age range. Thus, while this method allows for age- and gender-dependencies, the final "risk" will never be for the individual patient, but would be a nominal risk for a population of patients of similar gender and age.

APPENDIX A
LAR MODEL (EPA) FOR BREAST CANCER

As mentioned in Chapter 5, pg. 52, for estimates of LAR of breast cancer mortality the EPA uses a very different method than that employed by BEIR VII. The methodology is much more complex than the one for risk of breast cancer incidence and thus the following write-up was taken directly from the Blue Book (pgs. 44-47) (*17*) to explain it. The section details EPA's method and compares the results with the BEIR VII method. The only things changed in the write-up were the equation and table numbers to match the format of this paper.

Let $M_I(D,e,a_I)$ denote the EAR for incidence at attained age a_I from an exposure at age *e*. If *da* represents an infinitesimally small age increment, the probability of a radiogenic cancer between ages a_I and (a_I + *dt*) would be:

$$f_{D,e}(a_I)da = M_I(D,e,a_I)\,S(a_I)/S(e)da\,. \qquad \text{(A-1)}$$

For the cancer to result in a death at age $a_M > a_I$, the patient would have to survive the interval (a_I, a_M), and then die from the cancer at age a_M. This and the concept of the relative survival rate form the basis for the method. The relative survival rate for a breast cancer patient would be the ratio of the survival rate for the patient divided by the expected survival rate (without breast cancer). Assume the relative survival depends only on the length of the time interval and the age of diagnosis. Let $t = a_M - a_I$, and let $R(t, a_I)$ be the relative survival function. Then the probability of survival with breast cancer for the interval (a_I, a_M) is $S(a_M)/S(a_I)R(t,a_I)$.

Suppose the breast cancer mortality rate (h) among those with breast cancer depends on the age of diagnosis but does not depend on other factors, such as whether the cancer is

radiogenic, or on attained age. Then the proba-bility of a radiogenic breast cancer death between ages a_M and (a_M + da) can be shown to equal:

$$f_{D,e}(a_M)da = \left(\frac{1}{S(e)} \int_{e+L}^{a_M} h(a_M)\, M_I(D,e,a_I)\, S(a_M) R(t,a_I)\, da_I \right) da\,. \qquad \text{(A-2)}$$

The LAR for breast cancer mortality for an exposure at age e is:

$$LAR(D,e) = \int_{e+L}^{110} f_{D,e}(a_M)\, da_M\,, \qquad \text{(A-3)}$$

and Equation A-4 is applied as before to calculate the LAR for the U.S. population.

$$LAR(D, stationary) = \frac{\int_0^{110-L} S(e) \cdot LAR(D,e) \cdot de}{\int_0^{110-L} S(e)\, de} \qquad \text{(A-4)}$$

For these calculations, we used the 5-y relative survival rates given in Table A-1 (*21*) and assumed that breast cancer mortality rates (for those with breast cancer) depend only on age at diagnosis and are equal to:

$$h(a_I) = -(0.2) \log R(5, a_I) \qquad \text{(A-5)}$$

It should be noted that results from several studies indicate that, for most stages, breast cancer mortality rates are not highly dependent on time since diagnosis – at least for the first 10 years (*22, 23*). Thus, for these calculations, we assumed that relative survival rates depend on time since diagnosis as in Equation A-6.

$$R(t, a_I) = \exp[-t \cdot h(a_I)] \qquad \text{(A-6)}$$

Table A-1. Female breast cancer cases and 5-y relative survival rates by age of diagnosis for 12 SEER areas, 1988-2001[1]

Age (y)	Cases	Relative Survival Rates (%)
20-34[2]	6,802	77.8
35-39	12,827	83.5
40-44	24,914	88.0
45-49	33,784	89.5
50-54	34,868	89.5
55-59	32,701	89.6
60-64	32,680	90.1
65-69	34,435	91.0
70-74	32,686	91.8
75-79	27,134	91.4
80-84	17,475	90.7
85+	12,457	86.6
Total	302,763	89.3

[1]Adapted from Table 13.2 in Ries et al. (*21*)
[2]For ages of exposure < 20, 5-y relative survival rate of 77.8% was assumed.

Based on the method just outlined, the LAR for breast cancer mortality is 0.95×10^{-2} Gy^{-1}. This is about 30% larger than in BEIR VII. Much of the discrepancy between the two sets of results can be attributed to observed increases in breast cancer incidence rates and declines in mortality rates. From 1980 to 2000, age-averaged breast cancer incidence rates (per 100,000 women) increased by about 35% (102.2 to 136.0), whereas the mortality rates declined by about 15% (31.7 to 26.6) (*24*).

To understand the effect these trends in incidence and mortality have on the BEIR VII LAR projection for mortality, recall the BEIR VII formula:

$$M(D,e,a) = EAR(D,e,a)\frac{\lambda_M(a)}{\lambda_I(a)} \ . \qquad \text{(A-7)}$$

The underlying assumptions are that: a) the absolute risk of radiogenic cancer death from an exposure at age e is equal to the absolute risk of a radiation-induced cancer multiplied by a lethality ratio (that depends on attained age) and b) lethality ratios can be approximated by

current mortality to incidence rate ratios. However, since the time between breast cancer diagnosis and death is relatively long, lethality rates might be better approximated by comparing current mortality rates to incidence rates observed for (much) earlier time periods. If, as data indicate, current incidence rates are considerably higher than in the past, the BEIR VII denominator is too large, and the estimated lethality ratio is too small. This would result in a downward bias in the BEIR VII projection for mortality.

Our projection has limitations which must be noted. First, its validity depends on the extent to which estimates of relative survival functions can be used to approximate mortality rates from breast cancer for people with breast cancer. Long-term survival rates for breast cancer patients are desirable for constructing valid estimates for this approach, but since these survival rates can change rapidly, there is considerable uncertainty in extrapolating rates for periods beyond 5-10 y. Finally, reduced expected survival among breast cancer patients may be partly attributable to causes other than breast cancer. For example, if some breast cancers are related to obesity, breast cancer patients as a group may be at greater risk of dying from cardiovascular disease.

APPENDIX B
DESCRIPTION OF ADDITIONAL CANCER SITE MODELS NOT IN EPA

The following write-up was provided by Dr. David Pawel from the U.S. EPA (Radiation Protection Division) which explains the derivation of the models used for the following sites: oral cavity, kidney, pancreas, gallbladder, central nervous system (CNS), esophagus, rectum, and new "other solid" (or remainder) mentioned in Chapter 5, pg. 57. As mentioned in Chapter 5, the kidney is included in the Blue Book but under a different methodology. The only things changed in the write-up were the equation and table numbers to match the format of this paper.

BEIR VII's risk model for what are often termed "residual site" cancers deserves special mention. The residual category generally includes relatively rare cancers for which data from the LSS cohort or other epidemiological studies was judged to be insufficient for reliable quantification of radiogenic site-specific risks. For these sites, the BEIR VII Committee pooled data from the LSS cohort to obtain stable estimates of risk. With only slight modification, the same pooling-of-data approach for residual site cancers was used for EPA's Blue Book. However, this approach can be problematic for medical applications, for which doses often depend greatly on cancer site and cancer site-specific doses are needed.

Here, an approach, very similar to the one described in Pawel, et al. (*25*), was used to obtain separate estimates of risk for the following 7 cancer sites: brain and central nervous system (CNS), esophagus, kidney, gallbladder, oral, pancreas, and rectum.

First, data from the lifespan study (LSS) cohort on cancer incidence for about 80,000 the A-bomb survivors were analyzed to obtain estimates of ERR for each of these sites. The analysis employed essentially the same Poisson regression techniques, as described in Breslow and Day (*26*) and the report by Preston et al. (*27*). The software program Epicure (*28*) was used for calculations. The same type of model used in BEIR VII for ERR was fit using data for these

7 specific cancer sites, i.e., ERR depends on dose (D), cancer site (c), sex(s), age-at-exposure(e), and attained age (a):

$$ERR(D, s, e) = \beta_{c,s}\, D \exp\,[\gamma\,(e\text{-}30)/10]\,(a/60)^{\eta}, \qquad \text{(B-1)}$$

where

$$e^{*} = \frac{\min(e,30) - 30}{10}. \qquad \text{(B-2)}$$

The age-at-exposure and attained-age parameters were assumed to be the same for these sites (γ = -0.3, η = -4.1), and, for all 7 sites, ERR was assumed to be about 35% larger for females than males. Finally, empirical Bayes (EB) techniques were used to obtain the parameter estimates for the linear-dose-response parameters (β) given in Table B-1 – see Pawel et al. (*25*) for details. Poisson regression techniques were applied to data for "other solid" cancers, e.g. "residual site" cancers other than the 7 sites identified in Table B-1, to obtain the parameter estimates given in the last row of the table.

Table B-1. ERR parameter estimates for additional site-specifc cancers and "other solid"

Cancer Site	β (male)	β (female)	Age-at-exposure (γ)	Attained age (η)
CNS	0.132	0.179	-0.3	-4.1
Esophagus	0.129	0.175	-0.3	-4.1
Gallbladder	0.033	0.045	-0.3	-4.1
Kidney	0.119	0.160	-0.3	-4.1
Oral	0.132	0.179	-0.3	-4.1
Pancreas	0.125	0.169	-0.3	-4.1
Rectum	0.065	0.087	-0.3	-4.1
Other solid	0.479	1.192	-0.3	-1.4

Note: Parameters developed and provided by Dr. David Pawel from U.S. EPA, Radiation Protection Division

Projections of LAR were calculated using methods very similar to those described in the section General Methodology for Calculating Lifetime Attributable Risks (LAR). The ERR

were calculated using the parameter values given in Table B-1, and then applied both to a) U.S. baseline rates obtained from the SEER program, and b) baseline rates estimated from the Japanese LSS data. Final estimates of LAR were equal to 0.7 times the LAR estimates obtained using U.S. baseline rates and 0.3 times the LAR estimates based in the Japanese baseline rates. The final answer was adjusted down by a DDREF of 1.5.

APPENDIX C
DETAILS OF THE 18-F-FDG PET/CT SIMULATION

The following write-up was provided by Mike Wayson (Ph.D. candidate-Medical Physics, ALRADS) from the University of Florida for the PET portion of the simulation. The only things changed in the write-up were the equation and table numbers to match the format of this paper.

18-F-FDG Internal Dosimetry for the University of Florida Hybrid Computational Phantoms

Transport methods

Phantom preparation

Monte Carlo N-Particle eXtended version 2.6 (MCNPX v2.6) was used for the radiation transport simulations. MCNPX v2.6 cannot directly simulate radiation transport through continuous three-dimensional surfaces/volumes. As a result, the UF hybrid NURBS/PM phantoms were each reconstituted as a three-dimensional voxel array using an in-house MATLAB^{TM} code with each voxel assigned a unique organ ID.

Ideally, voxel resolutions would be isotropic and have dimensions equal to the skin thickness in each phantom. However, resulting phantom binary file sizes become too large to effectively simulate at these resolutions, so anisotropic voxel resolutions were derived. Only the UFH00M and UFH00F phantoms were able to be simulated at isotropic voxel resolutions equal to the skin thickness. Because of this, voxel dimensions were selected to optimize voxel resolution and total voxel matrix size for all other phantoms. The final voxel dimensions and matrix sizes are in Table C-1.

Skin and lymphatic nodes are not explicitly modeled in NURBS/PM format, so these structures were added after the voxelization process was complete. Skin was added using an in-house MATLAB^{TM} code which replaces the outermost voxel layer with skin voxels. Lymphatic

nodes were placed using a code detailed in Lee et al. (*29*). The voxelized versions of the UF phantoms were then incorporated into MCNPX by repeated structures syntax. Physical characteristics and descriptions of the UF phantom family can be found in Lee et al. (*30*).

Table C-1. UF phantom family voxel dimensions and matrix sizes.

Phantom	Voxel Resolution (cm)			Number of Voxels			Total Matrix Size (x 10^7)
	X-direction	Y-direction	Z-direction	X-direction	Y-direction	Z-direction	
UFH00MF	0.0663	0.0663	0.0663	350	215	720	5.42
UFH01MF	0.0663	0.0663	0.1400	396	253	550	5.51
UFH05MF	0.0850	0.0850	0.1928	416	235	576	5.63
UFH10MF	0.0990	0.0990	0.2425	428	226	580	5.61
UFH15M	0.1250	0.1250	0.2832	414	226	590	5.52
UFH15F	0.1200	0.1200	0.2828	410	238	574	5.60
UFHADM	0.1579	0.1579	0.2207	362	195	796	5.62
UFHADF	0.1260	0.1260	0.2700	390	241	610	5.73

Simulation details

The phantoms were described in MCNPX using lattice structures. A lattice file detailing, in raster fashion, the organ/tissue identification numbers of all voxels was accessed during simulation. Unique tissue densities and material compositions were assigned to between 153 (UFH15M) and 179 (UFH00M) structures in the phantoms. Internal sources were simulated through the creation of "source files". These files were generated using an in-house MATLAB^{TM} code and specify the voxel coordinates of all voxels associated with the source tissue. Sources were simulated as uniformly distributed throughout the source tissue. Source tissues for ^{18}F-FDG were the brain, heart wall, liver, lungs, urinary bladder contents, and a single source compartment called "all other tissues" defined to be all body tissues less the defined source tissues, air in the body, and walled organ contents (*31*).

Energy deposition was tracked during transport for all non-skeletal target tissues of interest, accounting for all photons and electrons generated during the simulation down to a cutoff energy of 1 keV. For the beta particle simulations, energy deposition was also tracked in the spongiosa and medullary cavities to account for primary beta dose to the radiosensitive skeletal tissues. Volume-averaged photon fluence was recorded over all spongiosa and medullary cavity sites for application of recently developed skeletal photon dose response functions (DRFs) to account for skeletal dose enhancement from photon interactions in the skeletal microstructure (*32*). Doses to radiosensitive tissues as identified by ICRP Publication 103 and the BEIR VII report were calculated using the skeletal photon DRFs, and all target tissues can be seen in Table C-2.

Table C-2. Target tissues simulated for all phantoms.

Target Tissues	
BEIR VII	ICRP 103
Active marrow	Bladder
Bladder	Bone-marrow (red)
Breast (female only)	Bone surfaces
Central Nervous System and Brain	Brain
Colon	Breast
Esophagus	Colon
Gall bladder	Gonads - Ovaries
Kidney	Gonads - Testes
Liver	Liver
Lung	Lung
Oral Cavity	Oesophagus
Ovary	Remainder Tissues**
Pancreas	Salivary glands
Prostate	Skin
Rectum	Stomach
Remainder*	Thyroid
Skin	
Stomach	
Thyroid	
Total shallow marrow	
Uterus	

**Small intestine, digestive system (organs not already listed), nasal cavity, respiratory system (organs not already listed), thymus, renal pelvis, connective tissue, testes, all other tissues.
** Adrenals, extrathoracic (ET) region, gall bladder, heart, kidneys, lymphatic nodes muscle oral mucosa, pancreas, prostate, small intestine, spleen, thymus, and uterus/cervix.

F-18 is a pure positron emitter, and the decay spectrum was taken from ICRP Publication 107 (*33*). For direct spectrum sampling, all energies were simulated, and the relative probability of selecting a particular energy was set to the yield at that energy. Annihilation photons were accounted for in a separate simulation. One hundred million particle histories were simulated. The Integrated Tiger Series (ITS)-style electron energy indexing algorithm was used. Simulations were performed at the University of Florida's Advanced Laboratory for Radiation Dosimetry Studies (ALRADS) on a PSSC Labs (Lake Forest, CA) blade cluster running sixty-four 2 GHz processors with 2 GB of memory per processor.

Internal dose calculation

To calculate the radiation absorbed dose to all tissues of interest, the MIRD Pamphlet No. 21 internal dosimetry schema was used and is given in Equations C-1 and C-2 (*34*).

$$D(r_T) = \sum_{r_S} \left[\int_0^\infty A(r_S, t)\,dt \right] S(r_T \leftarrow r_S) = \sum_{r_S} \tilde{A}(r_S)\, S(r_T \leftarrow r_S) \tag{C-1}$$

$$S(r_T \leftarrow r_S) = \sum_i \frac{E_i Y_i \phi(r_T \leftarrow r_S; E_i)}{m_T} = \sum_i \Delta_i SAF(r_T \leftarrow r_S; E_i) \tag{C-2}$$

where $\tilde{A}(r_S)$ is the time-integrated activity or the total number of nuclear transformations occurring in source tissue r_S, $S(r_T \leftarrow r_S)$ is the radionuclide S value, defined as the mean absorbed dose rate to target tissue r_T per unit activity in source tissue r_S, E_i is the energy of the i^{th} radiation, Y_i is the yield of the i^{th} radiation, $\phi(r_T \leftarrow r_S; E_i)$ is the absorbed fraction (AF) defined as the fraction of radiation energy emitted by the i^{th} radiation from source tissue r_S that is absorbed in target tissue r_T, m_T is the mass of the target tissue r_T, Δ_i is the delta value for the i^{th} radiation, defined as the product of the energy and the yield of the i^{th} radiation, and $\text{SAF}(r_T \leftarrow r_S; E_i)$ is the specific absorbed fraction (SAF), defined as the ratio of the AF to the target tissue mass.

Measures of energy deposition in the target tissues of interest were given in units of MeV, so the final values of energy deposition calculated by MCNPX were divided by the average initial energy of the radiation simulated and the mass of the target to obtain the SAF for the source-target combination of interest. Since the whole spectrum was simulated directly, the summation operator in Equation C-2 disappeared, and Equation C-2 assumed the form of Equation C-3. The direct simulation SAF inherently accounts for all radiation emissions and their relative contributions to the final dose.

$$S(r_T \leftarrow r_S) = \sum_k \bar{E}_k \cdot Y_k \cdot SAF(r_T \leftarrow r_S)_k \tag{C-3}$$

where $S(r_T \leftarrow r_S)$ is the radionuclide S value, $\bar{E}_k$ is the average energy of emission for radiation type *k*, Y_k is the total yield of radiation type *k*, and $\mathrm{SAF}(r_T \leftarrow r_S)_k$ is the single SAF value for the direct spectrum simulation of radiation type *k*.

For skeletal target tissues, photon contribution to dose was calculated by applying skeletal photon DRFS using Equation C-4.

$$SAF(r_T \leftarrow r_S)_k = \frac{C}{\bar{E}_k} \sum_j w(r_T)_j \sum_i \left[\frac{D(r_T)}{\Phi(E_i)} \right] \Phi(j \leftarrow r_S; E_i)_k \tag{C-4}$$

where *C* is a unit conversion constant, $\bar{E}_k$ is the average energy of emission for radiation type *k*, $w(r_T)_j$ is the mass fraction of the target tissue r_T in bone site *j*, $D(r_T)/\Phi(E_i)$ is the skeletal photon DRF for target tissue r_T at photon energy E_i, $\Phi(j \leftarrow r_S; E_i)_k$ is the photon fluence emitted from source tissue r_S incident on the spongiosa/medullary cavity of bone site *j* for photons of energy E_i from radiation type *k*, and $SAF(r_T \leftarrow r_S)_k$ is the SAF for target tissue r_T from source tissue r_S for radiation type *k*.

Doses to the radiosensitive tissues in the skeleton from the annihilation photons were completely accounted for by the skeletal photon DRFs since no primary beta particles were

involved. However, the skeletal tissue doses from the primary beta particle simulations were calculated by including contributions from both primary beta particles and photons created during transport (e.g. bremsstrahlung photons). Since there are no appreciable dose enhancement effects attributed to electron energy deposition in bone, it was assumed that the doses to active marrow and total shallow marrow were equal to the absorbed dose in the spongiosa and medullary cavities. Therefore, the energy deposition results from the beta particle simulations in spongiosa and medullary cavities were divided by the average initial energy of the beta spectrum and the mass of the spongiosa or medullary cavity site where the energy deposition was tracked. Skeletal averaged dose to these tissues was calculated as the mass weighted average of doses to the individual bone sites. Volume-averaged photon fluence was also tracked during beta transport, and skeletal photon DRFs were subsequently applied. The final dose to the active marrow and total shallow marrow was calculated as the sum of these two dose measure results.

Uncertainties for 1584 energy deposition tallies due to annihilation photons ranged from 0% to 45% with an average of 1.4%. Uncertainties for 1656 energy deposition tallies due to beta particles ranged from 0% to 100% with an average of 16.4%. While some of the uncertainties from the beta particle simulations were quite high, the target tissues displaying these high uncertainties did not receive appreciable dose from the beta particles. Any dose recorded was a result of photon (non-annihilation) cross-dose resulting from the primary beta particles. Uncertainties associated with primary beta dose, magnitudes that were comparable to the annihilation photon doses, were generally good (<5%).

Biokinetic information was taken from ICRP Publication 106 (*31*). Residence times per unit administered activity (AA) for ^{18}F-FDG were given in units of hours for all source tissues

and can be seen in Table C-3. Residence times for "all other tissues" included contributions from the urinary bladder contents even though a unique residence time was given for the urinary bladder. Therefore, the "urinary bladder contents" tissue was treated separately, and the residence time for the "all other tissues" compartment was adjusted by subtracting out the age-dependent residence times for the urinary bladder contents. No value was given for the newborn, so the 1-year-old urinary bladder contents residence time was assigned to the newborn. Doses to all target tissues per unit administered activity (AA) were calculated using Equation C-1. Typical AAs for pediatric whole-body ^{18}F-FDG PET/CT were determined using information from Gelfand et al. (*35*). Adult guidelines were also given in the study by Gelfand et al. (*35*). The average adult AA was 555 MBq, so the adult male and female AAs were designed to average to the recommended average AA but reflect the difference in phantom mass. The recommendations for ^{18}F-FDG are in Table C-4, and the calculated AAs are in Table C-5.

Table C-3. Biokinetic data for ^{18}F-FDG.

Organ (S)	F_s	T (h)	a	$\tilde{A}_s/A_0$(h)
Brain	0.08	∞	1.0	0.21
Heart wall	0.04	∞	1.0	0.11
Lungs	0.03	∞	1.0	0.079
Liver	0.05	∞	1.0	0.13
Other organs and tissues	0.80	0.20	0.075	1.7
		1.5	0.225	
		∞	0.70	
Urinary bladder contents	0.24			
Adult, 15 years, 10 years				0.26
5 years				0.23
1 year				0.16

Note: taken from ICRP Publication 106 (*31*)

Table C-4. Recommended AAs for pediatric and adult patients.

	Minimum	Maximum	Average	Minimum Total (MBq)
Pediatric (MBq/kg)	3.70	5.20	4.45	37
Adult (MBq)	370	740	555	

Note: taken from ICRP Publication 107 (*33*)

Table C-5. Calculated AAs for the UF phantom family (MBq).

	Newborn	1-year-old	5-year-old	10-year-old	15-year-old	Adult
Male	37.0	51.6	91.8	168.6	297.7	610.3
Female	37.0	51.6	91.8	168.5	275.5	499.7

The following write-up was provided by Daniel Long (MS Student-Medical Physics, ALRADS) from the University of Florida for the CT portion of the simulation.

Computed Tomography (CT) External Dosimetry for PET/CT Exams

Organ doses for the computed tomography (CT) portion of the PET/CT exam were calculated for each hybrid computational phantom using an organ dose database generated using a custom Monte Carlo source term within Monte Carlo N-Particle extended version 2.6 (MCNPX v2.6). The source term modeled a Siemens Somatom Sensation 16 CT scanner, which provides CT imaging for the Siemens Biograph 16 PET/CT scanner, and was described in a study by Lee et al (*36*). The source term had previously been validated using both CTDI and anthropomorphic phantom measurements, and was used to generate a large set of MCNPX organ doses for individual axial beam slices spanning the entire length of each hybrid computational phantom. Multiple sets of axial slice organ doses were calculated to account for each beam energy, beam filtration, and computational phantom combination. The age-dependent CT scan parameters for these simulated PET/CT exams were taken from a paper, written by Alessio et al (*37*), regarding whole-body PET/CT protocols. A summary of these scan parameters can be found in Table C-6.

Table C-6. Scan parameters for the CT simulation

	Phantom					
Scan Parameter	Newborn	1 Year	5 Year	10 Year	15 Year	30 Year
Beam Energy (kVp)	120	120	120	120	120	120
Beam Collimation (cm)	2.4	2.4	2.4	2.4	2.4	2.4
Effective mAs	10	15	20	25	30	35
Pitch	0.984	0.984	0.984	0.984	0.984	0.984
Scan Length (cm)	30.4	44.3	59.5	75.5	94.6	104.7

Notes: Anatomical Landmarks of Scan: Base of skull to mid-thigh

To simulate exams, the appropriate single axial slice MCNPX doses were first summed along the entire anatomical scan length (from the base of the skull to the mid-thigh for all

phantoms). Since MCNPX provides organ dose calculation results in dose per simulated photon, the number of photons delivered by the scanner per unit mAs, called the Monte Carlo normalization factor, were multiplied to the MCNPX dose results to obtain organ doses in absolute units. The normalization factors were calculated based on the ratio of pencil ion chamber measurements in free-in-air (mGy/mAs) to MCNPX-simulated free-in-air ion chamber doses (mGy/photon) that had previously been made. Absolute organ doses for each individual scan could then be calculated by multiplying the dose in mGy/mAs by the total mAs delivered during the exam. This total axial scan dose was then divided by the specified pitch for the exam to approximate doses from a helical CT scan.

APPENDIX D
SITE-SPECIFIC ORGAN DOSES AND EFFECTIVE DOSES OBTAINED FROM THE MEDICAL SIMULATION

Table D-1. Organ equivalent doses in mSv obtained for males from the PET component of the simulation

	Organ Equivalent Doses (mSv)					
(Males)	Age-at-exposure					
Site	Newborn	1 Year	5 Year	10 Year	15 Year	30 Year
Stomach	5.91	2.98	2.88	3.10	3.35	7.15
Colon	5.65	2.99	2.94	3.08	3.71	6.95
Liver	8.79	4.54	4.89	6.16	7.27	13.61
Lung	10.28	4.99	4.67	5.39	5.58	11.37
Urinary Bladder	17.30	12.01	10.85	14.25	17.12	33.74
Thyroid	5.31	2.59	2.35	2.38	2.60	5.01
Bone	4.58	2.34	2.38	2.69	2.95	6.19
Skin	3.64	1.66	1.66	1.71	1.84	3.60
Oral Cavity	5.18	2.49	2.33	2.33	2.51	5.42
Kidney	5.67	2.78	2.80	2.83	3.14	6.43
Pancreas	5.64	2.78	2.84	3.13	3.38	6.77
Gallbladder	6.05	3.07	3.17	3.59	4.18	8.24
CNS/Brain	5.55	2.55	3.42	5.63	8.94	20.79
Esophagus	6.04	2.96	3.13	3.42	3.75	7.81
Rectum	5.81	2.78	3.75	5.00	5.66	7.42
Prostate	7.49	4.65	5.95	7.05	7.04	13.75
Active Marrow	4.59	2.23	2.31	2.90	3.49	7.27
Remainder	5.21	2.48	2.49	2.58	2.74	5.51

Notes:
*Doses to the Active Marrow are used for calculation of LAR of leukemia
*Dose for the 30 Year old were applied to individuals of age $\geq$ 30 years

Table D-2. Organ equivalent doses in mSv obtained for females from the PET component of the simulation

(Female)	Organ Equivalent Doses (mSv)					
	Age-at-exposure					
Site	Newborn	1 Year	5 Year	10 Year	15 Year	30 Year
Stomach	5.88	2.97	2.89	3.10	3.31	6.63
Colon	5.57	2.95	2.85	3.02	3.20	6.65
Liver	8.78	4.53	4.89	6.16	6.77	13.58
Lung	10.28	4.98	4.66	5.39	5.88	10.79
Urinary Bladder	17.08	12.41	10.77	14.36	17.68	32.63
Thyroid	5.42	2.54	2.34	2.36	2.55	5.12
Bone	4.56	2.34	2.36	2.66	2.99	5.50
Skin	3.63	1.66	1.66	1.71	1.82	3.52
Oral Cavity	5.13	2.30	2.39	2.43	2.57	5.84
Kidney	5.62	2.77	2.80	2.83	2.95	5.62
Pancreas	5.64	2.78	2.84	3.13	3.32	6.52
Gallbladder	6.20	3.13	3.18	3.60	4.22	7.89
CNS/Brain	5.55	2.55	3.42	5.63	8.93	18.90
Esophagus	6.10	2.98	3.13	3.44	3.54	7.04
Rectum	5.56	2.89	2.97	3.75	5.99	10.42
Breast	4.03	2.25	2.31	2.43	2.72	5.13
Ovary	6.31	4.24	5.40	6.89	8.34	14.23
Uterus	7.76	7.18	6.17	8.31	9.11	14.97
Active Marrow	4.57	2.22	2.28	2.85	3.46	6.52
Remainder	5.20	2.48	2.47	2.58	2.72	5.33

Notes:

*Doses to the Active Marrow are used for calculation of LAR of leukemia

*Dose for the 30 Year old were applied to individuals of age ≥ 30 years

Table D-3. Organ equivalent doses in mSv obtained for males from the CT component of the simulation

(Males)	Organ Equivalent Doses (mSv)					
	Age-at-exposure					
Site	Newborn	1 Year	5 Year	10 Year	15 Year	30 Year
Stomach	1.45	1.96	2.35	2.54	2.64	2.56
Colon	1.45	1.96	2.51	2.84	2.56	3.15
Liver	1.52	2.10	2.57	2.90	2.37	3.24
Lungs	1.45	2.18	2.64	2.76	2.82	2.97
Urinary Bladder	1.46	2.02	2.59	2.65	3.24	2.84
Thyroid	1.83	2.61	3.69	4.43	3.99	6.16
Bone	1.18	1.53	2.10	2.14	2.15	1.99
Skin	1.11	1.35	1.44	1.73	1.82	2.04
Oral cavity	1.50	1.78	2.14	2.81	3.36	3.41
Kidney	1.52	2.08	2.66	2.56	3.19	2.27
Pancreas	1.44	1.91	2.34	2.40	2.60	2.17
Gall bladder	1.42	1.94	2.46	2.88	2.27	2.78
CNS/Brain	0.42	0.43	0.59	0.76	0.81	0.89
Esophagus	1.35	2.10	2.54	2.59	2.78	2.58
Rectum	1.29	2.08	2.76	2.73	4.24	2.94
Prostate	1.29	1.92	2.53	2.63	3.55	2.86
Active marrow	1.14	1.49	1.48	1.82	2.33	2.00
Remainder	1.32	1.67	1.98	2.28	2.48	2.67

Notes:
*Doses to the Active Marrow are used for calculation of LAR of leukemia
*Dose for the 30 Year old were applied to individuals of age $\geq$ 30 years

Table D-4. Organ equivalent doses in mSv obtained for females from the CT component of the simulation

(Female)	Organ Equivalent Doses (mSv)					
	Age-at-exposure					
Site	Newborn	1 Year	5 Year	10 Year	15 Year	30 Year
Stomach	1.45	1.97	2.36	2.56	3.43	3.04
Colon	1.45	1.96	2.52	2.85	3.12	2.76
Liver	1.52	2.10	2.57	2.91	2.65	2.56
Lungs	1.45	2.18	2.64	2.76	2.76	2.91
Urinary Bladder	1.47	2.02	2.60	2.75	2.55	2.59
Thyroid	1.83	2.61	3.68	4.42	5.21	4.88
Bone	1.18	1.53	2.10	2.14	2.10	2.60
Skin	1.11	1.35	1.44	1.73	1.84	2.12
Oral cavity	1.45	1.71	2.07	2.73	3.68	3.29
Kidney	1.52	2.08	2.67	2.57	2.62	3.59
Pancreas	1.44	1.91	2.34	2.40	2.68	3.00
Gall bladder	1.42	1.95	2.46	2.90	2.50	2.43
CNS/Brain	0.42	0.42	0.59	0.76	0.99	1.07
Esophagus	1.35	2.10	2.54	2.60	2.66	2.79
Rectum	1.29	2.09	2.78	2.71	2.20	2.42
Breast	1.35	1.61	1.91	2.49	2.54	2.11
Ovaries	1.33	1.84	2.30	2.31	2.28	2.23
Uterus	1.30	1.77	2.23	2.23	2.10	2.15
Active marrow	1.14	1.49	1.48	1.82	2.06	2.40
Remainder	1.32	1.67	1.98	2.28	2.32	2.72

Notes:

*Doses to the Active Marrow are used for calculation of LAR of leukemia

*Dose for the 30 Year old were applied to individuals of age ≥ 30 years

Table D-5. Effective dose in mSv obtained from the PET simulation

Effective Dose (mSv)					
Age-at-exposure					
Newborn	1 Year	5 Year	10 Year	15 Year	30 Year
6.93	3.68	3.75	4.34	5.01	9.46

Note: Effective dose calculated using doses obtained from PET simulation and tissue weighting factors from ICRP 103

Table D-6. Effective dose in mSv obtained from the CT simulation

Effective Dose (mSv)					
Age-at-exposure					
Newborn	1 Year	5 Year	10 Year	15 Year	30 Year
1.48	2.04	2.48	2.81	2.90	3.19

Note: Effective dose calculated using doses obtained from CT simulation and tissue weighting factors from ICRP 103

APPENDIX E
CANCER RISKS OBTAINED FROM THE 18-F-FDG PET/CT SIMULATION

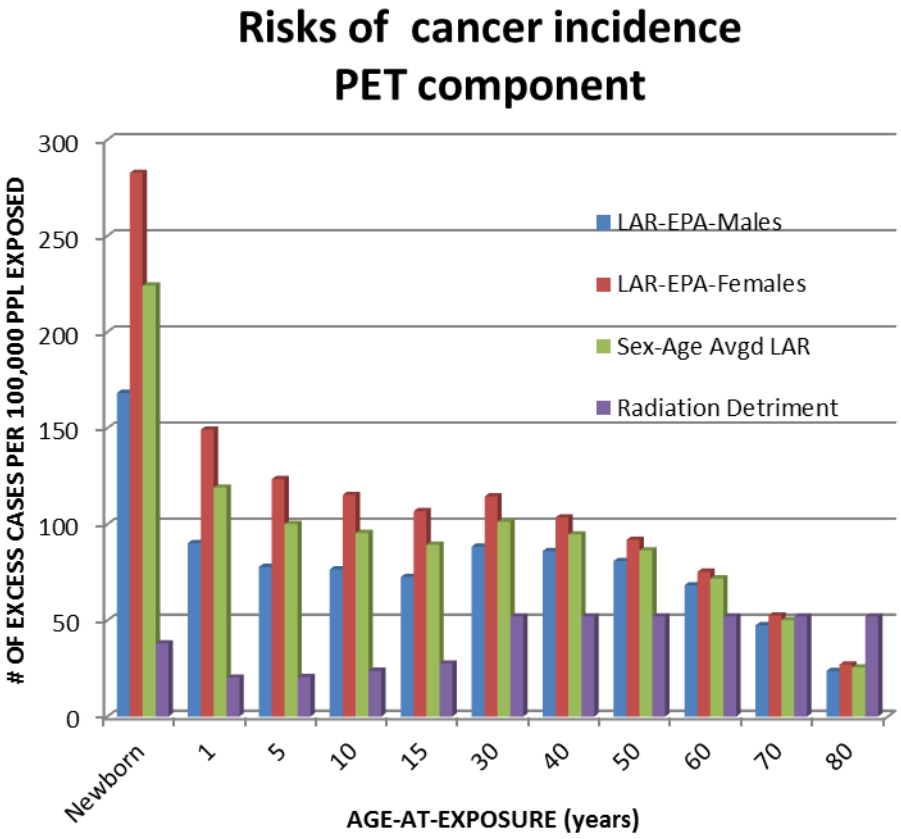

Figure E-1. Lifetime attributable risks of cancer incidence and radiation detriment from the PET component of the simulation

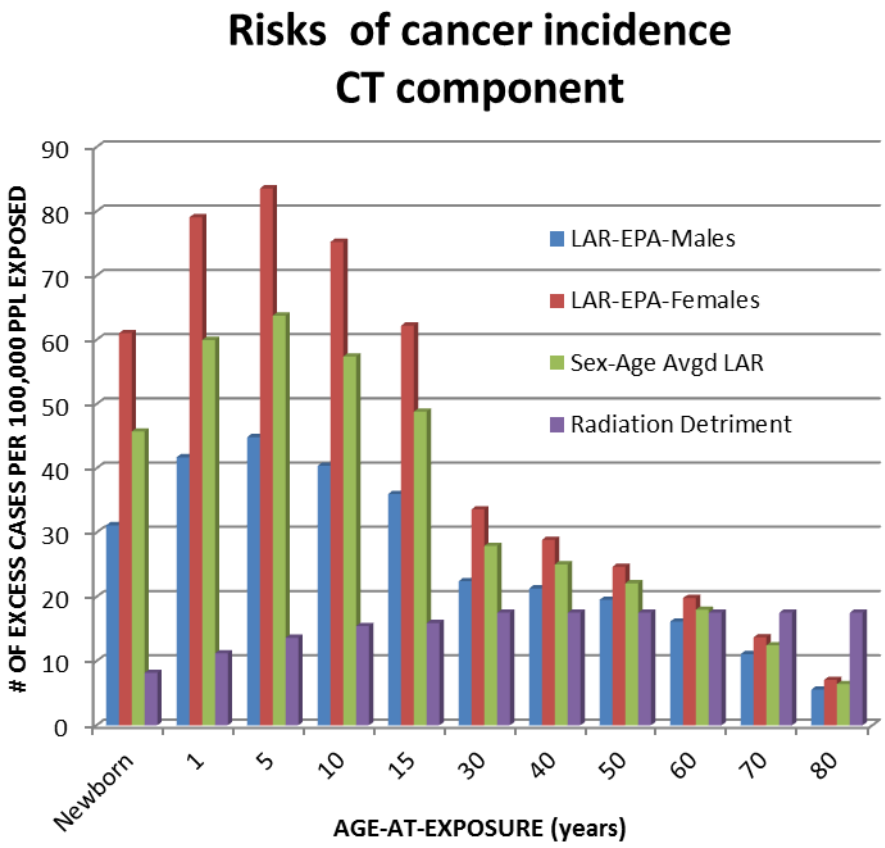

Figure E-2. Lifetime attributable risks of cancer incidence and radiation detriment from the CT component of the simulation

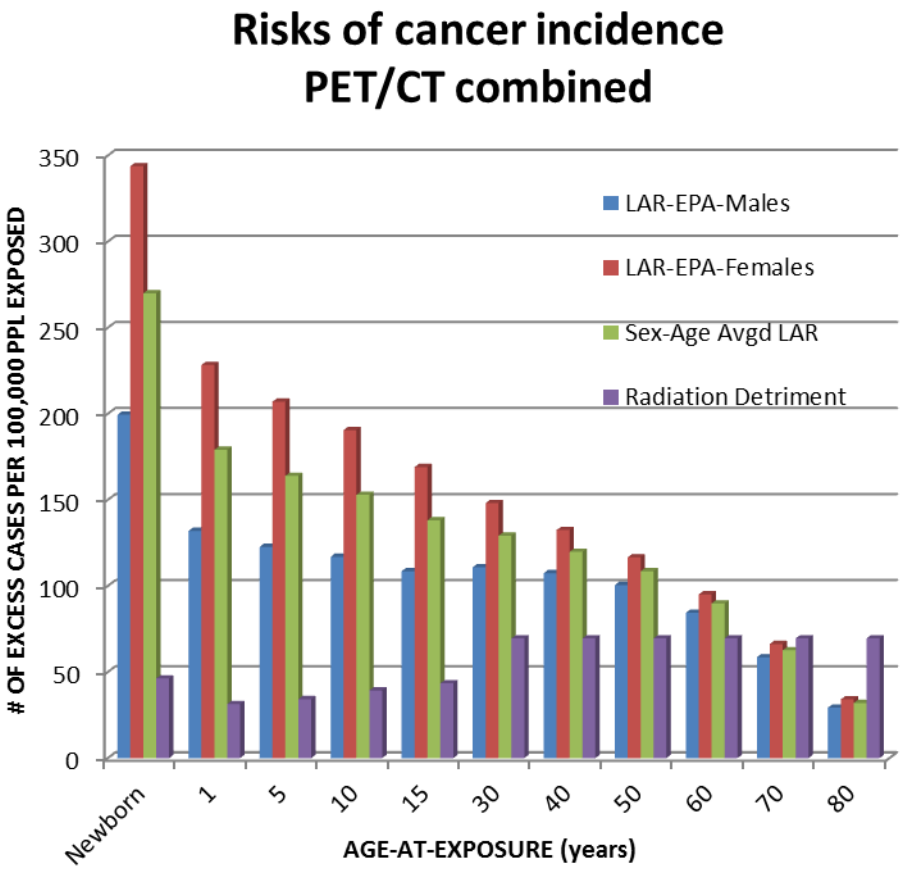

Figure E-3. Combined (PET/CT) lifetime attributable risks of cancer incidence and radiation detriment

Table E-1. Cancer incidence and mortality risks obtained by applying the doses acquired from the PET simulation

Age at exposure	Cancer Incidence Risk			Cancer Mortality Risk			Rad. Detriment
	LAR_{EPA}[a] (Male)	LAR_{EPA} (Female)	LAR_{AVG}[b]	LAR_{EPA} (Male)	LAR_{EPA} (Female)	LAR_{AVG}	ICRP-103[c]
Newborn	168	283	224	77	140	108	38
1	90	149	119	39	71	55	20
5	78	123	100	33	60	46	21
10	77	115	96	33	57	45	24
15	73	107	89	31	53	42	28
30	88	115	101	38	59	49	52
40	86	104	95	38	56	47	52
50	81	92	86	37	52	44	52
60	68	75	72	34	46	40	52
70	47	53	50	28	35	32	52
80	24	27	26	17	21	20	52

Note: Number of excess cases for a population of 100,000 persons. Age-at-exposure in years

[a] Overall sex-and-age specific lifetime attributable risk of cancer (incidence or mortality) using EPA LAR revised models. LAR of skin cancer incidence was not included in the Cancer Incidence Risk estimates

[b] Overall sex-and-age averaged lifetime attributable risk of cancer (incidence or mortality) using EPA LAR revised models

[c] Radiation detriment calculated from the effective dose as defined by ICRP 103 (*10*)

Table E-2. Fractional cancer incidence and mortality risks – PET simulation

Age at exposure	Fractional Risk Cancer Incidence			Fractional Risk Cancer Mortality			Fractional Rad. Det.
	LAR_{EPA} (Male)	LAR_{EPA} (Female)	LAR_{AVG}	LAR_{EPA} (Male)	LAR_{EPA} (Female)	LAR_{AVG}	ICRP-103
Newborn	1.9	3.2	2.5	2.0	3.6	2.8	1.0
1	1.0	1.7	1.3	1.0	1.8	1.4	0.5
5	0.9	1.4	1.1	0.9	1.6	1.2	0.5
10	0.9	1.3	1.1	0.8	1.5	1.2	0.6
15	0.8	1.2	1.0	0.8	1.4	1.1	0.7
30	1.0	1.3	1.1	1.0	1.5	1.3	1.4
40	1.0	1.2	1.1	1.0	1.5	1.2	1.4
50	0.9	1.0	1.0	1.0	1.4	1.2	1.4
60	0.8	0.9	0.8	0.9	1.2	1.0	1.4
70	0.5	0.6	0.6	0.7	0.9	0.8	1.4
80	0.3	0.3	0.3	0.5	0.6	0.5	1.4

Note: risks as ratios of each of the risks to the risk for the 30-year old adult male (from incidence, mortality, and detriment separately). Age-at-exposure in years

Table E-3. Cancer incidence and mortality risks obtained by applying the doses acquired from the CT simulation

Age at exposure	Cancer Incidence Risk			Cancer Mortality Risk			Rad. Detriment
	LAR_{EPA}[a] (Male)	LAR_{EPA} (Female)	LAR_{AVG}[b]	LAR_{EPA} (Male)	LAR_{EPA} (Female)	LAR_{AVG}	ICRP-103[c]
Newborn	31	61	46	14	27	21	8
1	42	79	60	19	36	27	11
5	45	84	64	20	38	29	14
10	40	75	57	19	35	27	15
15	36	62	49	17	30	23	16
30	22	34	28	11	18	14	18
40	21	29	25	11	17	14	18
50	20	25	22	10	15	13	18
60	16	20	18	9	13	11	18
70	11	14	12	7	10	9	18
80	6	7	6	5	6	5	18

Note: Number of excess cases for a population of 100,000 persons. Age-at-exposure in years
[a] Overall sex-and-age specific lifetime attributable risk of cancer (incidence or mortality) using EPA LAR revised models. LAR of skin cancer incidence was not included in the Cancer Incidence Risk estimates
[b] Overall sex-and-age averaged lifetime attributable risk of cancer (incidence or mortality) using EPA LAR revised models
[c] Radiation detriment calculated from the effective dose as defined by ICRP 103 (10)

Table E-4. Fractional cancer incidence and mortality risks – CT simulation

Age at exposure	Fractional Risk Cancer Incidence			Fractional Risk Cancer Mortality			Fractional Rad. Det.
	LAR_{EPA}[a] (Male)	LAR_{EPA} (Female)	$LAR_{S,A}$[b]	LAR_{EPA}[c] (Male)	LAR_{EPA} (Female)	$LAR_{S,A}$	ICRP-103[d]
Newborn	1.4	2.7	2.0	1.3	2.5	1.9	0.7
1	1.9	3.5	2.7	1.7	3.3	2.5	1.0
5	2.0	3.7	2.8	1.9	3.4	2.6	1.2
10	1.8	3.4	2.6	1.7	3.2	2.4	1.4
15	1.6	2.8	2.2	1.5	2.7	2.1	1.5
30	1.0	1.5	1.2	1.0	1.6	1.3	1.6
40	0.9	1.3	1.1	1.0	1.5	1.2	1.6
50	0.9	1.1	1.0	0.9	1.4	1.2	1.6
60	0.7	0.9	0.8	0.9	1.2	1.0	1.6
70	0.5	0.6	0.6	0.7	0.9	0.8	1.6
80	0.2	0.3	0.3	0.4	0.5	0.5	1.6

Note: risks as ratios of each of the risks to the risk for the 30-year old adult male (from incidence, mortality, and detriment separately). Age-at-exposure in years

Table E-5. Total cancer incidence and mortality risks obtained from the ^{18}F-FDG PET/CT simulation combined

Age at exposure	Cancer Incidence Risk			Cancer Mortality Risk			Rad. Detriment
	LAR_{EPA}[a] (Male)	LAR_{EPA} (Female)	LAR_{AVG}[b]	LAR_{EPA} (Male)	LAR_{EPA} (Female)	LAR_{AVG}	ICRP-103[c]
Newborn	199	344	270	91	168	129	46
1	132	228	179	58	107	82	31
5	123	207	164	54	97	75	34
10	117	191	153	52	92	71	39
15	109	169	138	48	83	65	43
30	111	148	129	49	77	63	70
40	107	132	120	49	72	61	70
50	101	117	109	47	67	57	70
60	84	95	90	43	59	51	70
70	59	66	63	35	45	40	70
80	29	34	32	22	27	25	70

Note: Number of excess cases for a population of 100,000 persons. Age-at-exposure in years
[a] Overall sex-and-age specific lifetime attributable risk of cancer (incidence or mortality) using EPA LAR revised models. LAR of skin cancer incidence was not included in the Cancer Incidence Risk estimates
[b] Overall sex-and-age averaged lifetime attributable risk of cancer (incidence or mortality) using EPA LAR revised models
[c] Radiation detriment calculated from the effective dose as defined by ICRP 103 (10)

Table E-6. Fractional cancer incidence and mortality risks – PET/CT simulation

Age at exposure	Fractional Risk Cancer Incidence			Fractional Risk Cancer Mortality			Fractional Rad. Det.
	LAR_{EPA}[a] (Male)	LAR_{EPA} (Female)	$LAR_{S,A}$[b]	LAR_{EPA}[c] (Male)	LAR_{EPA} (Female)	$LAR_{S,A}$	ICRP-103[d]
Newborn	1.8	3.1	2.4	1.8	3.4	2.6	0.9
1	1.2	2.1	1.6	1.2	2.2	1.7	0.6
5	1.1	1.9	1.5	1.1	2.0	1.5	0.7
10	1.1	1.7	1.4	1.0	1.9	1.4	0.8
15	1.0	1.5	1.2	1.0	1.7	1.3	0.9
30	1.0	1.3	1.2	1.0	1.6	1.3	1.4
40	1.0	1.2	1.1	1.0	1.5	1.2	1.4
50	0.9	1.1	1.0	1.0	1.4	1.2	1.4
60	0.8	0.9	0.8	0.9	1.2	1.0	1.4
70	0.5	0.6	0.6	0.7	0.9	0.8	1.4
80	0.3	0.3	0.3	0.4	0.6	0.5	1.4

Note: risks as ratios of each of the risks to the risk for the 30-year old adult male (from incidence, mortality, and detriment separately). Age-at-exposure in years

LIST OF REFERENCES

1. Hall EJ, and Giaccia AJ. Radiobiology for the Radiologist. Philadelphia, PA: Lippincott Williams & Wilkins; 2006.

2. Brenner DJ. Effective dose: a flawed concept that could and should be replaced. *Br J Radiol*. 2008; 81:521-523.

3. National Council on Radiation Protection and Measurements (NCRP). *Ionizing Radiation Exposure of the Population of the United States*. Report No. 160. Bethesda, MD: NCRP; 2009.

4. Brenner DJ, Elliston CD, Hall EJ, et al. Estimated Risks of Radiation-Induced Fatal Cancer from Pediatric CT. *AJR*. 2001; 176:289–296.

5. Sgouros G, Frey EC, Bolch WE, et al. An Approach for Balancing Diagnostic Image Quality with Cancer Risk: Application to Pediatric Diagnostic Imaging of ^{99m}Tc-Dimercaptosuccinic Acid. *J Nucl Med*. 2011; 52:1923-1929.

6. International Commission on Radiological Protection (ICRP). *Recommendations of the International Commission on Radiological Protection*. ICRP Publication 26. Oxford, U.K.: Pergamon Press; 1977.

7. Nuclear Regulatory Commission (NRC) on the Internet. 2011. *Quality factor*. 07 Nov. 2011. < http://www.nrc.gov/reading-rm/basic-ref/glossary/quality-factor.html>

8. International Commission on Radiological Protection (ICRP). *Limits for Intakes of Radionuclides by Workers.* ICRP Publication 30. Oxford, U.K.: ICRP; 1979.

9. Bolch WE. Class Lecture. Radiation Dosimetry. *Radiation Dosimetry Quantities & Units.* University of Florida, Gainesville, FL. 06-07 Jan 2010.

10. International Commission on Radiological Protection (ICRP). *Limits for Intakes of Radionuclides by Workers.* ICRP Publication 60. Oxford, U.K.: Pergamon Press; 1990.

11. International Commission on Radiological Protection (ICRP). 2007 Recommendations of the International Commission on Radiological Protection. ICRP Publication 103. *Ann ICRP*. 2007; 37:1-332.

12. International Commission on Radiation Protection (ICRP). Radiological Protection in Medicine. ICRP Publication 105. *Ann ICRP*. 2007; 37:1-63.

13. International Commission on Radiation Protection (ICRP). *Basic Anatomical and Physiological Data for Use in Radiological Protection: Reference Values*. ICRP Publication 89. Oxford, U.K.: Pergamon Press; 2002.

14. International Commission on Radiation Protection (ICRP). *Report of the Task Group on Reference Man*. ICRP Publication 23. Oxford, U.K.: Pergamon Press; 1975.

15. Li X, Samei E, Segars WP, et al. Patient-specific Radiation Dose and Cancer Risk for Pediatric Chest CT. *Radiology*. 2011; 259(3):862-874.

16. National Research Council (NRC). Committee on the Biological Effects of Ionizing Radiation. *Health Risks from Exposure to Low Levels of Ionizing Radiation: BEIR VII-Phase2*. Washington, DC: The National Academies Press; 2005.

17. U.S EPA (Environmental Protection Agency). EPA Radiogenic Cancer Risk Models and Projections for the U.S. Population. EPA Report 402-R-11-001. 2011. Washington, DC: U.S. EPA.

18. Microsoft. Microsoft Excel. Redmond, Washington: Microsoft, 2007. Computer Software.

19. United Nations Scientific Committee on the Effects of Atomic Radiation (UNSCEAR). 2008. *UNSCEAR 2006 Report to the General Assembly with Scientific Annexes*. *Volume I. Effects of Ionizing Radiation.* New York: United Nations.

20. Anderson RN, and DeTurk PB. United States Life Tables. National Vital Statistics Reports. 2002; 50 (6):1-12. < www.cdc.gov/nchs/data/nvsr/nvsr50/nvsr50_06.pdf>

21. Ries LAG, Young JL, Keel GE, et al. *SEER Survival Monograph: Cancer Survival Among Adults: U.S. SEER Program, 1988-2001, Patient and Tumor Characteristics*. National Cancer Institute, SEER Program, NIH Pub. No. 07-6215, Bethesda, MD, 2007.

22. Bland KI, Menck HR, Scott-Conner CEH, et al. The national cancer data base 10-year survey of breast carcinoma treatment at hospitals in the United States. *Cancer.* 1998; 83:1262-1273.

23. Cronin K, Feuer E, Wesley M, et al. *Current Estimates for 5 and 10 Year Relative Survival.* Statistical Research and Applications Branch, National Cancer Institute. Technical Report #2003-04. 2003. Accessed 10/17/08 at < http://srab.cancer.gov/reports/tech2003.04.pdf>

24. Ries LAG, Melbert D, Krapcho M, DG *et al. SEER Cancer Statistics Review, 1975-2005*. National Cancer Institute. Bethesda, MD. Based on November 2007 SEER data submission, posted to the SEER website, 2008. <http://seer.cancer.gov/csr/1975_2005/>

25. Pawel D, Preston D, Pierce D, et al. Improved Estimates of Cancer Site-Specific Risks for A-Bomb Survivors . *Radiat Res*. 2008; 169:87-98.

26. Breslow NE, and Day NE. The Design and Analysis of Cohort Studies. International Agency for Research on Cancer. 1998. Lyon.

27. Preston DL, Ron E, Tokuoka S, et al. Solid cancer incidence in atomic bomb survivors: 1958-1998. *Radiat Res*. 2007; 168: 1-64.

28. Preston DL, Lubin JH, Pierce DA, et al. *Epicure User's Guide*. Hirosoft, Seattle, 1993.

29. Lee C, Pafundi DH, Kaufman K, et al. An algorithm for lymphatic node placement in hybrid computational phantoms - applications to radionuclide therapy dosimetry. *Proc IEEE.* 2009; 97(12):2098-2108.

30. Lee C, Lodwick D, Hurtado J, et al. The UF family of reference hybrid phantoms for computational radiation dosimetry. *Phys Med Biol.* 2010; 55(2):339-363.

31. International Commission on Radiation Protection (ICRP). Radiation Dose to Patients from Radiopharmaceuticals. ICRP Publication 106. *Ann ICRP*. 2008; 38(1-2):1-198.

32. Johnson PB, Bahadori AA, Eckerman KF, et al. Response functions for computing absorbed dose to skeletal tissues from photon irradiation-an update. *Phys Med Biol.* 2011; 56(8):2347-2365.

33. International Commission on Radiation Protection (ICRP). Nuclear Decay Data for Dosimetric Calculations. ICRP Publication 107. *Ann ICRP*. 2008; 38(3):e1-e26, 1-96.

34. Bolch WE, Eckerman KF, Sgouros G, et al. MIRD Pamphlet No. 21 – A generalized schema for radiopharmaceutical dosimetry: Standardization of nomenclature. *J Nucl Med.* 2009; 50(3):477-484.

35. Gelfand MJ, Parisi MT, Treves ST. Pediatric radiopharmaceutical administered doses: 2010 North American consensus guidelines. *J Nucl Med*. 2011; 52(2):318-322.

36. Lee C, Kim KP, Long D, et al. Organ doses for reference adult male and female undergoing computed tomography estimated by Monte Carlo simulations. *Med Phys*. 2011; 38:1196-1206.

37. Alessio AM, Kinahan PE, Manchanda V, et al. Weight-Based, Low-Dose Pediatric Whole-Body PET/CT Protocols. *J Nucl Med.* 2009; 50:1570-1578.

BIOGRAPHICAL SKETCH

Mr. Abadia arrived from Colombia to the United States in 2001 and completed his high-school education in this country. He received his Bachelor of Science degree in nuclear engineering from the University of Florida on May 2009. He is to receive his Master of Science degree in biomedical engineering with concentration on medical physics at the University of Florida on May 2012. He will begin working on his medical physics PhD soon after graduation. He is currently a member of the American Association of Physicists in Medicine (AAPM) and the Health Physics Society (HPS) and has served in the Society of Health and Medical Physics Students (SHMPS) at the University of Florida. His graduate research time has been primarily focused on studying alternative ways of stochastic risk quantification for radiogenic cancers from medical imaging procedures such as nuclear medicine, fluoroscopy, and computed tomography.